PRACE project PLepNuGam: a status report

R. Frezzotti and M. Garofalo

ETMC meeting, September 2019, Bonn

PLepNuGam: PRACE project (Rome123, Bonn) coordinated within ETMC on

Radiative leptonic decays of light and heavy pseudoscalar mesons from Lattice QCD

Focus here on: isospin symmetric $N_f = 2 + 1 + 1$ clover-Mtm-LQCD calculations

name	Nconf	κ	$a\mu_\ell$	μ_σ	μ_δ	β
cA211.53.24	4489 (620)	.1400645	0.0053	0.1408	0.1521	1.726
cA211.40.24	4882 (660)	.1400645	0.0040	0.1408	0.1521	1.726
cA211.30.32	4556 (280)	.1400645	0.0030	0.1408	0.1521	1.726
cA211.12.48	2368 (240)	.1400650	0.0012	0.1408	0.1521	1.726
cB211.25.48	4880 (300)	.1394267	0.0025	0.1246864	0.1315052	1.778
cB211.072.64	3164 (180)	.1394265	0.00072	0.1246864	0.1315052	1.778
cC211.06.80	1013 (100)	.1387510	0.0006	0.1060	0.1135	1.836

For isospin breaking corrections, including real γ's: F. Sanfilippo's talk

IB corrections evaluated on $N_f = 2 + 1 + 1$ Mtm-LQCD (old) ensembles.

Combining results @ $a \to 0$ info on $N_f = 1 + 1 + 1 + 1$ continuum QCD+QED

PLepNuGam: O(1/10) of the configurations analysed using spin-diluted sources 2-point correlators, with local-smeared and smeared-smeared for non-light mesons

[Comparison done with on-the-fly correlators (no dilution) for light-light mesons]

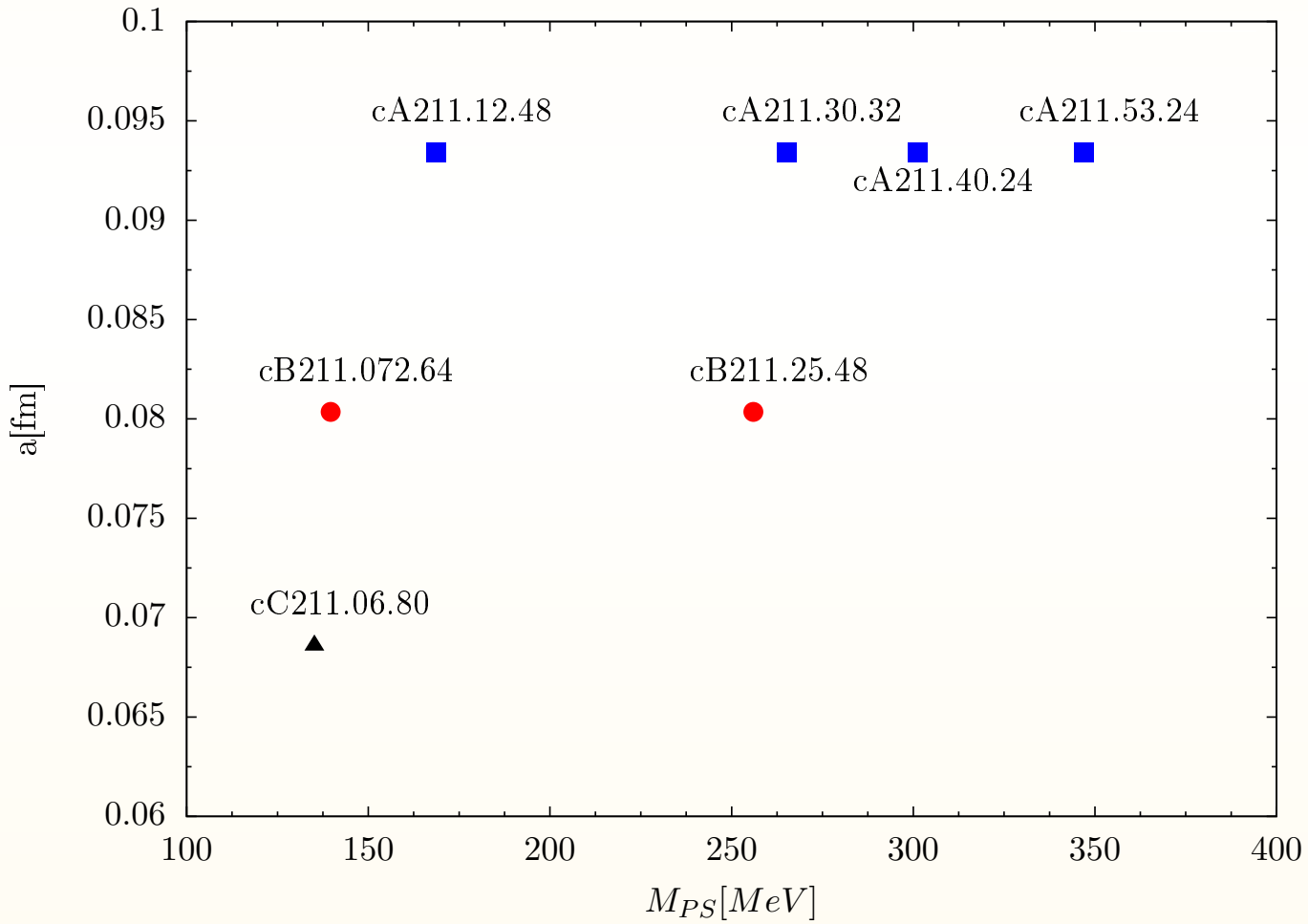

A few complementary analyses in the π, K and $D(D_s)$ sectors with encouraging preliminary results – for competitive precision still need

- few more ensembles (cB211.14.64, ...), possibly more correlators on L24, L32, L48
- having adequate FSE representation: larger dedicated ensembles cB211.25.24[32]
- disentangling smaller O(a^2) [clover] from small FSE for 1% accuracy
- quark mass RC with $< 1\%$ error (RI'-MOM: 3rd β to come ...)

[hadronic effects in (S)MOM schemes: ETMC2010 (M2-way), HPQCD 1909.00756]

- exploring/exploiting scale setting from Ω mass [compute w_0]
- indipendent cross-checks of the selected final analyses / error budget

- Finite volume effects:

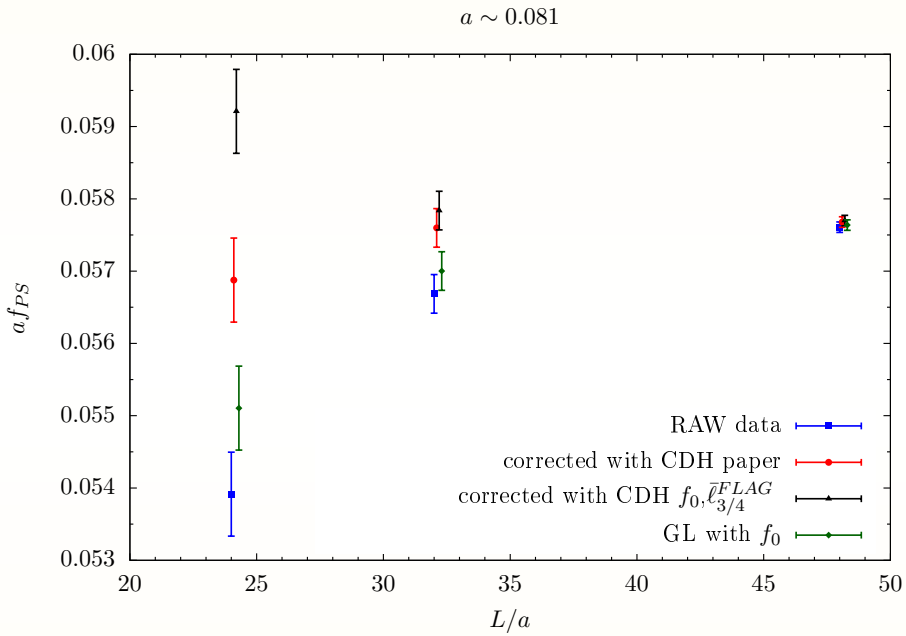

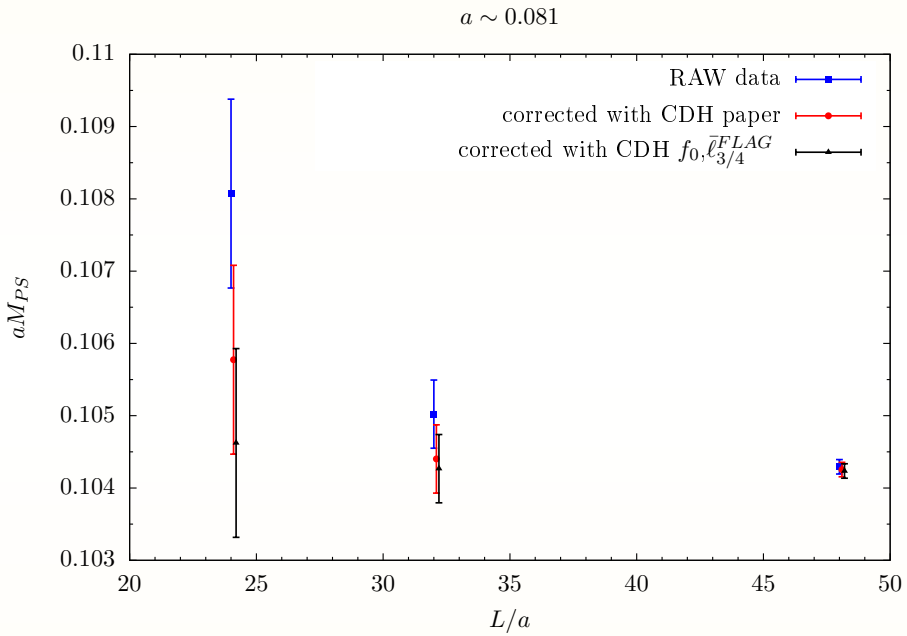

- Not yet enough precise data to establish the appropriate finite volume correction formulae

- Ensemble cA211.12.48: $m_{pcac}/\mu = -0.21(5)$
- Corrected for deviations from maximal twist

$$M_{PS}(m_{pcac}=0) = M_{PS}(m_{pcac})\left(1+\frac{m_{pcac}^2 Z_A^2}{\mu^2}\right)^{-1/4}$$

$$f_{PS}(m_{pcac}=0) = f_{PS}(m_{pcac})\left(1+\frac{m_{pcac}^2 Z_A^2}{\mu^2}\right)^{1/2}$$

where $f_{PS}(m_{pcac}) = 2a\mu_\ell \frac{a^2\langle 0|P_5^{local}|P\rangle}{aM_{PS}(m_{pcac})\sinh(aM_{PS}(m_{pcac}))}$

- Correction for deviations from maximal twist can also be estimated through reweighting: preliminary estimates agree with the formula above

•	$m_{pcac} \neq 0$	$m_{pcac} = 0$	reweighting
M_{PS}	0.08020(20)	0.08001(21)	0.07995(19)
f_{PS}	0.06089(24)	0.06146(24)	0.06154(95)

- The reweighting makes the error larger in f_{PS}

- PS-masses from

$$c(t) = \frac{1}{L^3} \sum_{\vec{x}} \langle \bar{Q}\gamma^5 Q(0) \bar{Q}\gamma^5 Q(x) \rangle$$

- Decay constant

$$af_P(\mu_1, \mu_2) = a(\mu_1 + \mu_2) \frac{a^2 \langle 0|P_5^{local}|P\rangle}{aM_P \sinh(aM_P)}.$$

- Analysis of full statistics ensembles measurements based on SU(2) ChPT:

$$(f_\pi w_0) \quad = (f w_0) \left[1 - 2\xi_l^M \log \xi_l^M + P_3 \xi_l^M + \frac{a^2}{w_0^2} P_4 \right] K_f^{FSE} \ ,$$

$$\xi_l^M = \frac{M_\pi^2}{16\pi^2 f^2}$$

- does not rely on the knowledge of the quark mass RC (Here Z_P)

Preliminary Results f_π

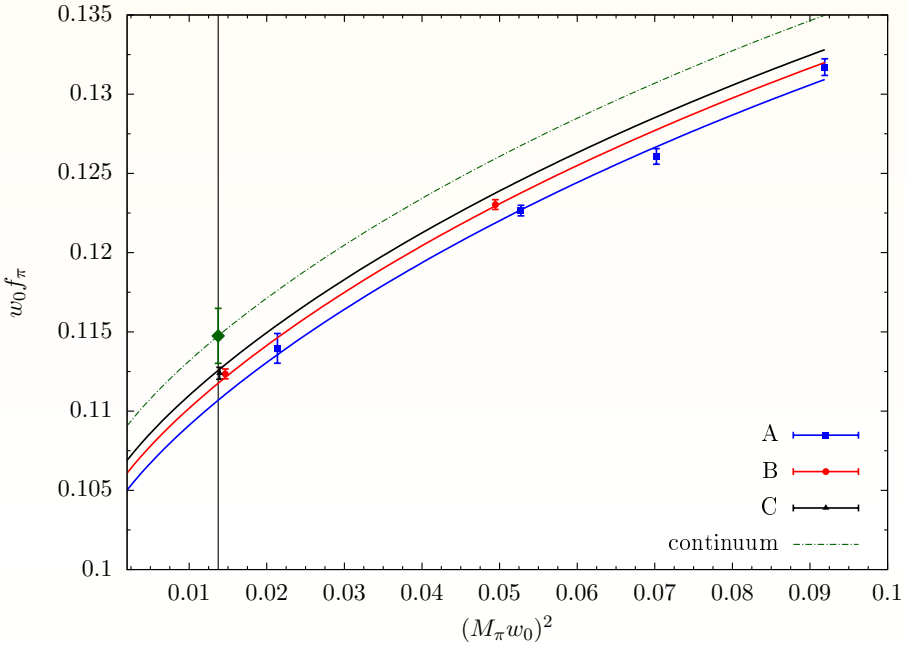

- Systematic error not included

$$f w_0 = (0.106046 \pm 0.0014) \quad \bar{\ell}_4 = (4.31888 \pm 0.12) \quad P4 = (-0.0534708 \pm 0.066)$$

Imposing $w_0 = 0.1714 \pm 0.0015$ fm [MILC, Phys. Rev. D 93, 094510] we get:

$$f_\pi = (130 \pm 2) MeV$$

Imposing $f_\pi = 130.41$

$$w_0 = (0.171161 \pm 0.0022) fm$$

K meson

- Interpolation in the meson mass M_K^2 of $f_K = A + BM_K^2$ for each ensemble at $(M_K^{ref} w_0)^2 = 0.1444, 0.1596, 0.1748$
- Chiral and continuum extrapolation for each $(M_K^{ref} w_0)^2$

$$f_k = P_1' \left[1 - \frac{3}{4} \xi_M \log \xi_M + P_2' \xi_M + P_4' a^2 \right] K_{f_K}^{FSE}$$

$$\xi_M = \frac{M_\pi^2}{16\pi^2 f^2}$$

- Interpolation in the meson mass M_K^2 of $f_K = A + BM_K^2$ at $a = 0$, $M_\pi = M_\pi^{exp}$
- $M_K^{exp} = \sqrt{\frac{M_{K^+}^2 + M_{K^0}^2}{2} - \frac{(1+\epsilon+2\epsilon_{K^0}-\epsilon_m)}{2}(M_{\pi^+}^2 - M_{\pi^0}^2)} = 494.2(4)\text{MeV}$
  [FLAG 2013, arXiv:1310.8555]

Preliminary results f_K

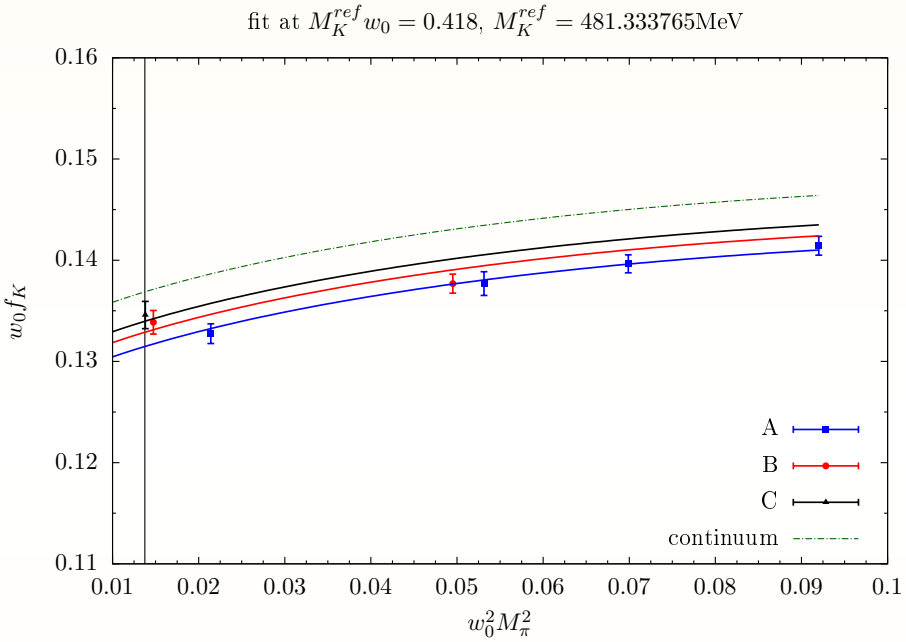

- Systematic error not included

$$f_K = (155.3 \pm 3.5) MeV$$

$$f_K/f_\pi = (1.19 \pm 0.02) MeV$$

Collaboration	Ref.	N_f	publication status	chiral extrapolation	continuum extrapolation	finite-volume errors	f_K/f_π	$f_{K^\pm}/f_{\pi^\pm}$
FNAL/MILC 17	[5]	2+1+1	A	★	★	★	$1.1980(12)(^{+5}_{-15})$	$1.1950(15)(^{+6}_{-18})$
ETM 14E	[35]	2+1+1	A	○	★	○	1.188(11)(11)	1.184(12)(11)
FNAL/MILC 14A	[18]	2+1+1	A	★	★	★		$1.1956(10)(^{+26}_{-18})$
ETM 13F	[253]	2+1+1	C	○	★	○	1.193(13)(10)	1.183(14)(10)
HPQCD 13A	[34]	2+1+1	A	★	○	★	1.1948(15)(18)	1.1916(15)(16)
MILC 13A	[254]	2+1+1	A	★	★	★		1.1947(26)(37)
MILC 11	[255]	2+1+1	C	○	○	○		$1.1872(42)^{\dagger}_{\text{stat.}}$
ETM 10E	[256]	2+1+1	C	○	○	○	$1.224(13)_{\text{stat}}$	
QCDSF/UKQCD 16	[40]	2+1	A	○	★	○	1.192(10)(13)	1.190(10)(13)
BMW 16	[39, 257]	2+1	A	★	★	★	1.182(10)(26)	1.178(10)(26)
RBC/UKQCD 14B	[10]	2+1	A	★	★	★	1.1945(45)	
RBC/UKQCD 12	[154]	2+1	A	★	○	★	1.199(12)(14)	
Laiho 11	[58]	2+1	C	○	★	○		$1.202(11)(9)(2)(5)^{\dagger\dagger}$
MILC 10	[37]	2+1	C	○	★	★		$1.197(2)(^{+3}_{-7})$
JLQCD/TWQCD 10	[258]	2+1	C	○	■	★	1.230(19)	
RBC/UKQCD 10A	[157]	2+1	A	○	○	★	1.204(7)(25)	
BMW 10	[38]	2+1	A	★	★	★	1.192(7)(6)	
MILC 09A	[17]	2+1	C	○	★	★		$1.198(2)(^{+6}_{-8})$
MILC 09	[128]	2+1	A	○	★	★		$1.197(3)(^{+6}_{-13})$
Aubin 08	[259]	2+1	C	○	○	○		1.191(16)(17)
RBC/UKQCD 08	[160]	2+1	A	○	■	★	1.205(18)(62)	
HPQCD/UKQCD 07	[36]	2+1	A	○	○	○	1.189(2)(7)	
MILC 04	[163]	2+1	A	○	○	○		1.210(4)(13)
ETM 14D	[260]	2	C	★	■	○	$1.203(5)_{\text{stat}}$	
ALPHA 13A	[261]	2	C	★	★	★	1.1874(57)(30)	
ETM 10D	[237]	2	C	○	★	○	$1.190(8)_{\text{stat}}$	
ETM 09	[41]	2	A	○	★	○	1.210(6)(15)(9)	
QCDSF/UKQCD 07	[262]	2	C	○	○	★	1.21(3)	

† Result with statistical error only from polynomial interpolation to the physical point.
†† This work is the continuation of Aubin 08.

FLAG 2019

D and D_s meson

- Interpolation in the meson mass M_D of $f_{D/D_s} = A + BM_D$ for each ensemble at three reference values $(M_D^{ref} w_0) = 1.2, 1.3, 1.4$
- Chiral and continuum extrapolation a

$$f_{D/D_s} = P_1(1 + P_2 M_\pi^2 + P_3 M_\pi^4 + P_4 a^2)$$

- Interpolation in the meson mass M_D of $f_{D/D_s} = A + BM_D$ at $a = 0$, $M_\pi = M_\pi^{exp}$
- $M_D^{exp} = \frac{M_{D^\pm} + M_{D^0}}{2} = 1.867\text{GeV}$
- In the D_s meson an extra interpolation in M_K^2 of $f_{D_s} = A + BM_K^2$ to $M_K^{exp} = 494.2(4)\text{MeV}$ is required

Preliminary results f_D and f_{D_s}

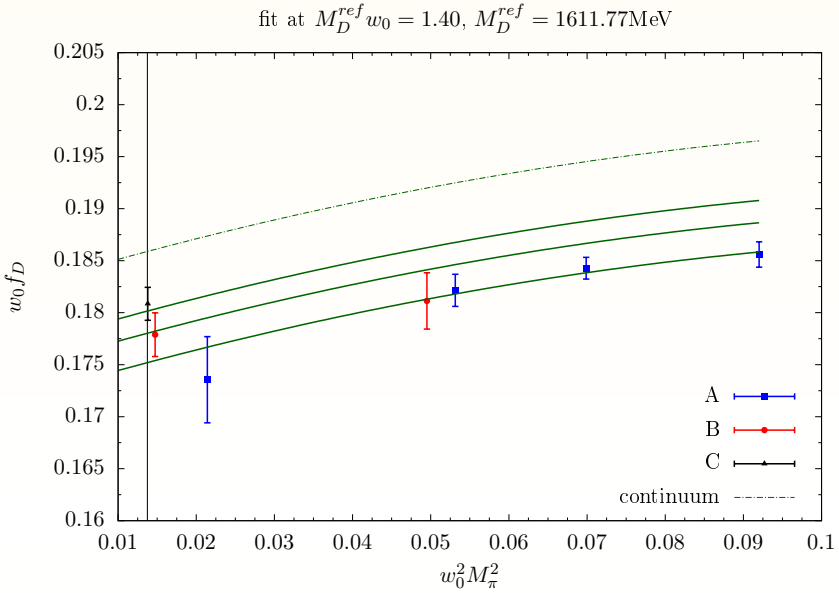

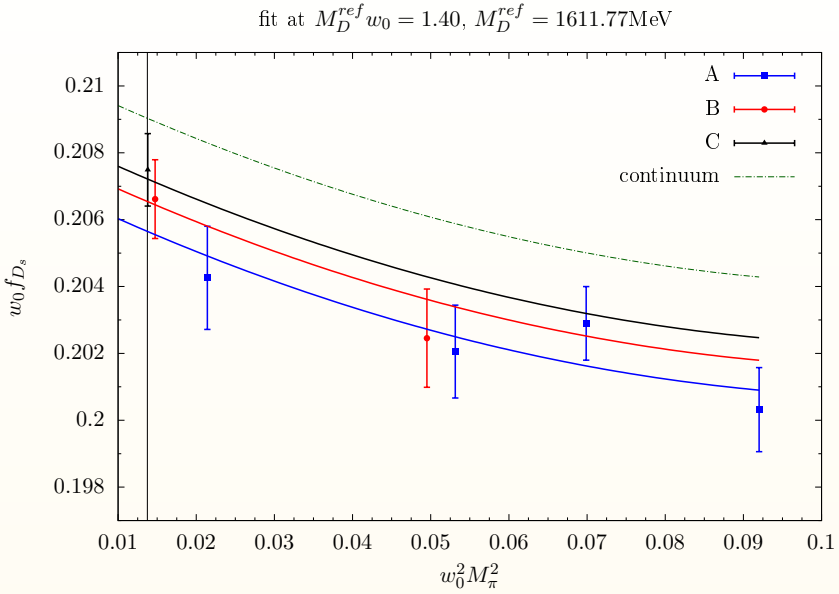

- Systematic error not included

$$f_D = (219 \pm 6) MeV$$
$$f_{D_s} = (246 \pm 3) MeV$$

Quark masses and Decay constants in Light, Strange ans Charm sectors from Nf=2+1+1 clover-Wtm simulations

ETMC Meeting Fall 2019

Bonn, September 23-25

Petros Dimopoulos

Introductory Remarks

- *Preliminary* analysis for quark masses ($m_{u/d}$, m_s and m_c) and decay constants (f_π, f_K, f_K/f_π, f_D, f_{Ds}/f_D and f_{Ds}).
- Employ the PLNG generated 2-point correlation functions (Local-Local, Smeared-Local, Smeared-Smeared).
- Employ data from $\beta = 1.726$ and 1.778 for which Z_P estimates are already available.
- Determination of Z_P at $\beta = 1.836$: ongoing work.
- Large parts of the analysis procedure in the Light sector concerning plateau choices and the combined fit analysis have already been under a cross-check process with Marco.

Ensemble Details

β	Ens.	(L,T)	$a\mu_\ell$	# meas.	w_0/a
1.726 ($a \simeq 0.093$ fm)	**A.12.48**	(48,96)	0.0012	240	1.8355(42)
	A.30.32	(32,64)	0.0030	280	
	A.40.24	(24,48)	0.0040	660	
	A.53.24	(24,48)	0.0053	620	
1.778 ($a \simeq 0.080$ fm)	B.072.64	(64,128)	0.00072	180	2.1347(47)
	B.25.48	(48,96)	0.0025	300	
	B.14.64	(64,128)	0.0014	-	
1.836 ($a \simeq 0.069$ fm)	**C.060.80**	(80,160)	0.00060	100	2.4884(36)

- **A.12.48** is (a bit) out of maximal twist: a correction factor has been implemented to M_{PS} and f_{PS} in the light and strange sectors. (See Notes delivered by Roberto and Silvano).
- **B.14.64**: configuration generation is on going (Bartek).
- **C.060.80** data have been used in a couple of test analyses as Z_P estimate at this β is still missing.
- A couple of simulations for controlling FSE are on going (Francesco).

Ensemble Details

β	Ens.	(L,T)	$a\mu_\ell$	# meas.	w_0/a
1.726 ($a \simeq 0.093$ fm)	**A.12.48**	(48,96)	0.0012	240	1.8355(42)
	A.30.32	(32,64)	0.0030	280	
	A.40.24	(24,48)	0.0040	660	
	A.53.24	(24,48)	0.0053	620	
1.778 ($a \simeq 0.080$ fm)	B.072.64	(64,128)	0.00072	180	2.1347(47)
	B.25.48	(48,96)	0.0025	300	
	B.14.64	(64,128)	0.0014	-	
1.836 ($a \simeq 0.069$ fm)	**C.060.80**	(80,160)	0.00060	100	2.4884(36)

- **w_0/a determination:**

for each β extrapolate the w_0/a estimates to the pion physical point using fit ansatz given by $(w_0/a)^2 = c_0 + c_1(M_{PS}/F_{PS})^2$. For each ensemble the values for w_0/a are obtained from the on-the-fly measurements,
see Bartek's `https://www.dropbox.com/s/bg0vaceq25mpahd/nf211_tmclover_run_statuses.tar.gz?dl=0`.
The results are still *preliminary*.

A Collection of (Preliminary) Results

	$m_{u/d}$ ($\overline{\text{MS}}$, 2 GeV) (MeV)	m_s ($\overline{\text{MS}}$, 2 GeV) (MeV)	$m_s/m_{u/d}$	m_c ($\overline{\text{MS}}$, 3 GeV) (GeV)
ETMC 19	3.46(22)	96.5(6.2)	27.92(35)	0.995(55)
FLAG 19	3.410(43)	93.12(69)	27.23(10)	0.987(11)

	f_π (MeV)	f_K (MeV)	f_K/f_π	f_D (MeV)	f_{Ds} (MeV)	f_{Ds}/f_D
ETMC 19	129.1(2.0)	155.0(2.2)	1.192(12)	214(5)	251(5)	1.173(25)
FLAG 19	130.2(0.2)	155.7(0.3)	1.1932(19)	212.0(7)	249.9(5)	1.1783(16)

- **ETMC 19** analysis employs data from 2 β's ($\beta = 1.726, 1.778$).
- For the results in the above Table $w_0 = 0.1714(15)$ by MILC (2+1+1 flavours), arXiv 1503.02769, has been employed.
- By setting the scale from f_π our analysis gives $w_0 = 0.1694(29)$ which is in good agreement with the corresponding MILC determination.
- Uncertainties are still large but are expected to be much reduced with the inclusion of the rest of the available data and in particular those from the third (fine) lattice spacing ($\beta = 1.836$) for which the Z_P estimate is not yet available.
- Better agreement for the quark masses between the **ETMC 19** *preliminary* central values and the **FLAG 19** results seems to be the case when RCs-M1 estimates are used.

Light sector -1

- Combined fit ansätze (SU(2) ChPT): (see ETMC arXiv:1403.4504)

$$(w_0 M_{\ell\ell})^2 = (2 w_0 B_0)(w_0 m_\ell)\left[1 + \xi_\ell log\xi_\ell + c_1\xi_\ell + c_2(a/w_0)^2\right] \mathrm{K}_M^{\mathrm{FSE}}$$

$$(w_0 f_{\ell\ell}) = (w_0 f_0)\left[1 - 2\xi_\ell log\xi_\ell + c_3\xi_\ell + c_4(a/w_0)^2\right] \mathrm{K}_f^{\mathrm{FSE}}$$

where: $\xi_\ell = (2B_0 m_\ell)/(4\pi f_0)^2$

- use correlation functions $C_{PP}(t)$ (Local-Local).
- $m_\ell = \mu_\ell / Z_P$.
- $af_{\mathrm{PS}} = 2a\mu_\ell \dfrac{|g_{\mathrm{PS}}|}{aM_{\mathrm{PS}} \sinh(aM_{\mathrm{PS}})}$

Light sector - 2

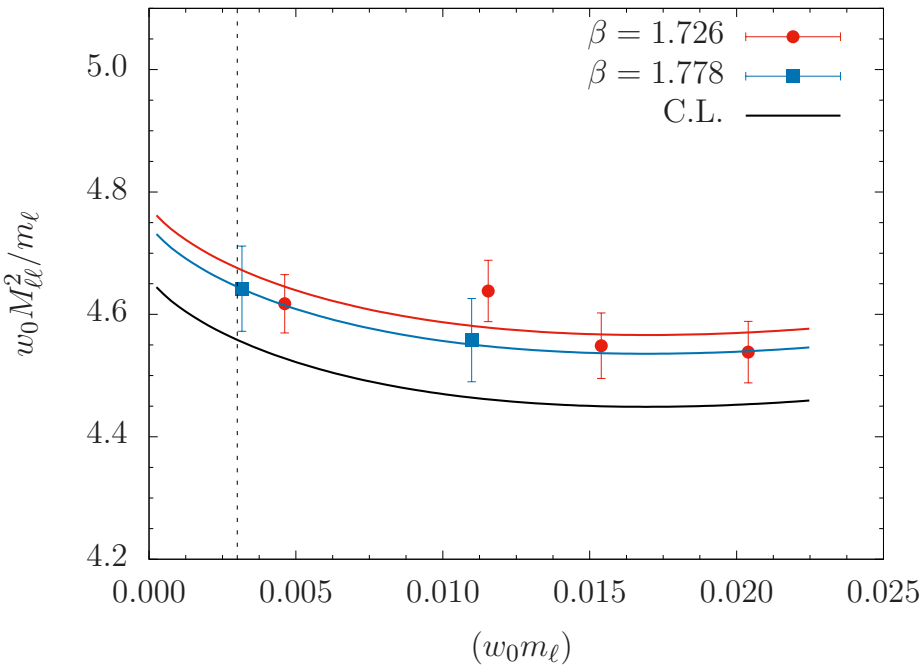

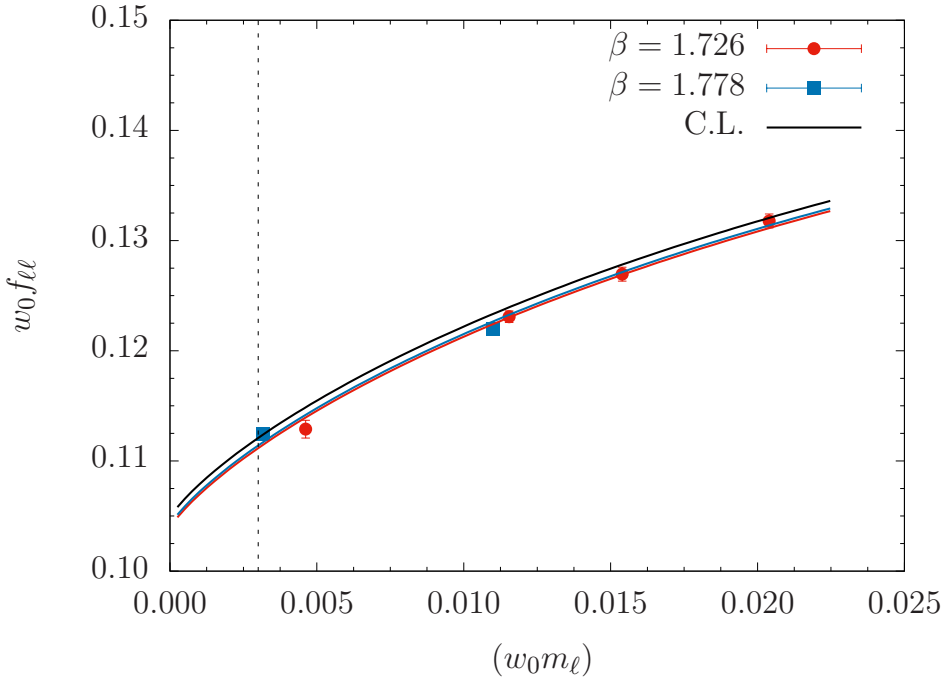

from combined fit:

$m_{ud}(\overline{\text{MS}}, 2\text{GeV}) = 3.46(22)$ MeV, $f_\pi = 129.1(2.0)$MeV; $\chi^2/\text{d.o.f.} = 2.3$.

- w/o correction for A.12.48:
$m_{ud}(\overline{\text{MS}}, 2\text{GeV}) = 3.51(22)$ MeV, $f_\pi = 130.3(2.0)$MeV; $\chi^2/\text{d.o.f.} = 2.7$

Light sector (include $\beta = 1.836$)

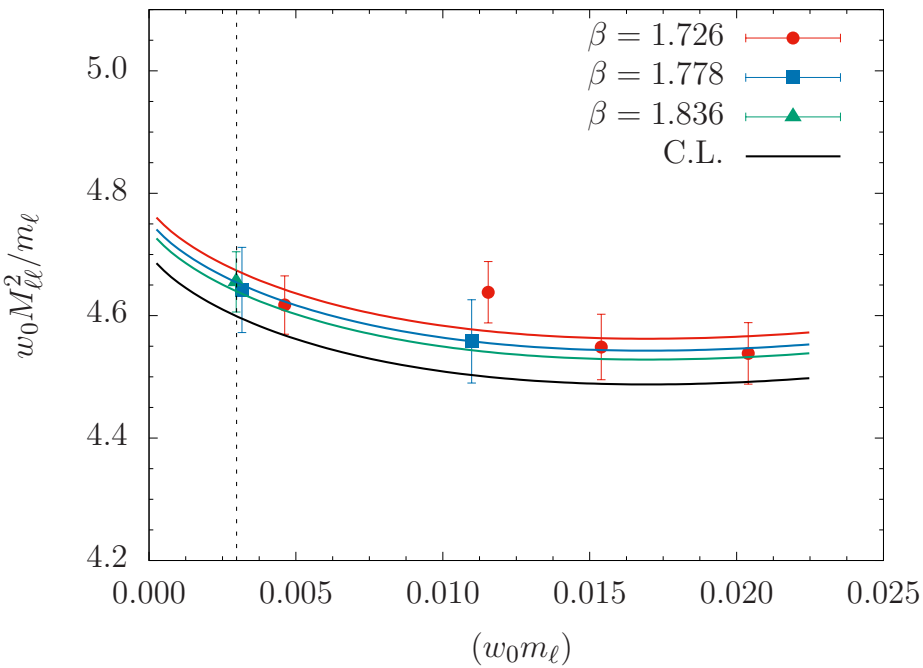

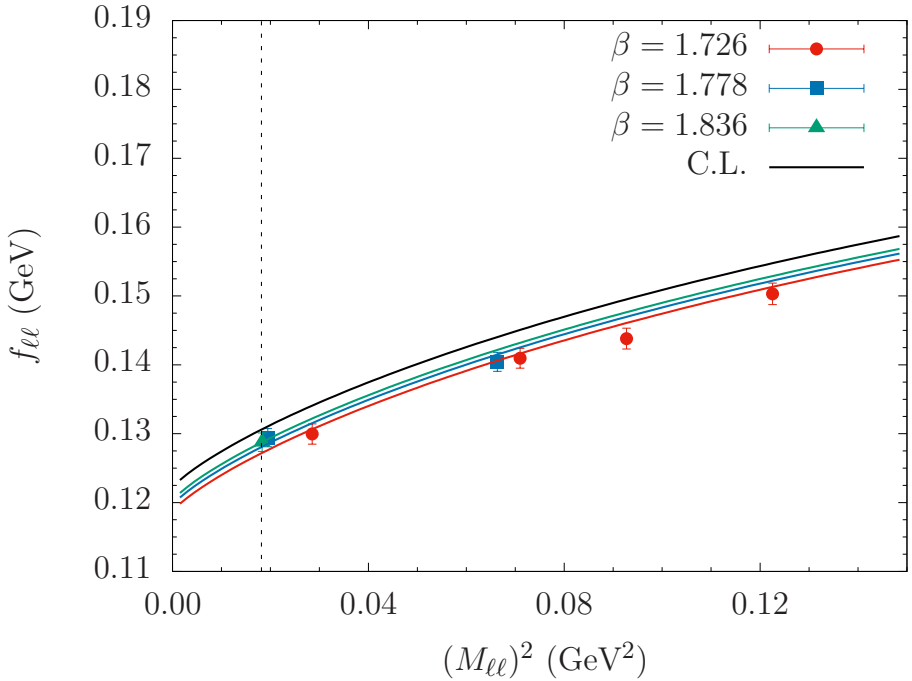

from combined fit:

$m_{ud}(\overline{\text{MS}}, 2\text{GeV}) = 3.43(11)$ MeV,

$f_\pi = 129.5(1.5)$MeV;

$\chi^2/\text{d.o.f.} = 1.8$.

$Z_P(\beta = 1.836)$ guessed.

SU(2) fit ansatz f_{ps} vs. M_{ps}^2:

$f_\pi = 130.6(1.9)$ MeV;

$\chi^2/\text{d.o.f.} = 0.35$

- compare w/o $\beta = 1.836$:
  $f_\pi = 130.7(2.4)$ MeV
  $\chi^2/\text{d.o.f.} = 0.44$

Light sector - collection of results for m_{ud}

Employing data from $\beta = 1.726$ & 1.778 and $w_0 = 0.1714(15)$ from MILC

Z_P	$m_{u/d}$ ($\overline{\text{MS}}$, 2 GeV) in MeV
M1 (subtr. $O(a^2 g_\star^2)$) [P.D.]	3.46(22)
M1 (subtr. $O(a_\infty g_0^2)$) [P.D.]	3.37(21)
M1 (subtr. $O(a^2 g_0^2)$) [P.D.]	3.52(30)
M1 (no subtr.) [P.D.]	3.36(22)
M1 (subtr. $O(a^2 g_0^2)$) [M.B.]	3.44(18)
M1 (subtr. $O(a^2 g_0^2)$) [E.F.]	3.44(25)
M2 (subtr. $O(a^2 g_\star^2)$) [P.D.]	3.65(18)
M2 (subtr. $O(a_\infty g_0^2)$) [P.D.]	3.71(20)
M2 (subtr. $O(a^2 g_0^2)$) [P.D.]	3.67(21)
M2 (no subtr.) [P.D.]	3.90(21)
M2a (subtr. $O(a^2 g_0^2)$) [E.F.]	3.66(19)
M2b (subtr. $O(a^2 g_0^2)$) [E.F.]	3.76(22)

- [P.D.] $\rightarrow$ Petros, [E.F.] $\rightarrow$ Enrico, [M.B.] $\rightarrow$ Mariane
- Difference between results obtained with methods M1 and M2 seems to be largerly reduced when data from the finest lattice spacing are included in the analysis ($Z_P(\beta = 1.836)$ guessed).

Strange sector - 1

- Fit ansätze (SU(2) ChPT):

(see ETMC arXiv:1403.4504 & arXiv:1411.7908)

$$1a.\quad (w_0 M_{\ell s})^2 = (w_0 B_0)[w_0(m_\ell + m_s)]\left[1 + c_1 m_\ell + c_2 (a/w_0)^2\right] \mathrm{K}_M^{\mathrm{FSE}}$$

$$1b.\quad (w_0 M_{\ell s})^2 = \left[C_0(m_s) + C_1(m_s) m_\ell\ (+C_2(m_s) m_\ell^2) + C_3 (a/w_0)^2\right] \mathrm{K}_M^{\mathrm{FSE}}$$

$$2.\quad (w_0 f_{\ell s}) = (w_0 P_0)\left[1 - (3/4)\xi_\ell log \xi_\ell + P_1 \xi_\ell + P_2 (a/w_0)^2\right] \mathrm{K}_f^{\mathrm{FSE}}$$

where: $\xi_\ell = (2 B_0 m_\ell)/(4\pi f_0)^2$

- use correlation functions $C_{PP}(t)$ (Local-Local).
- $m_{\ell,s} = \mu_{\ell,s}/Z_P$.
- $a f_{\mathrm{PS}} = (a\mu_\ell + a\mu_s) \dfrac{|g_{\mathrm{PS}}|}{a M_{\mathrm{PS}} \sinh(a M_{\mathrm{PS}})}$

Strange sector - 2

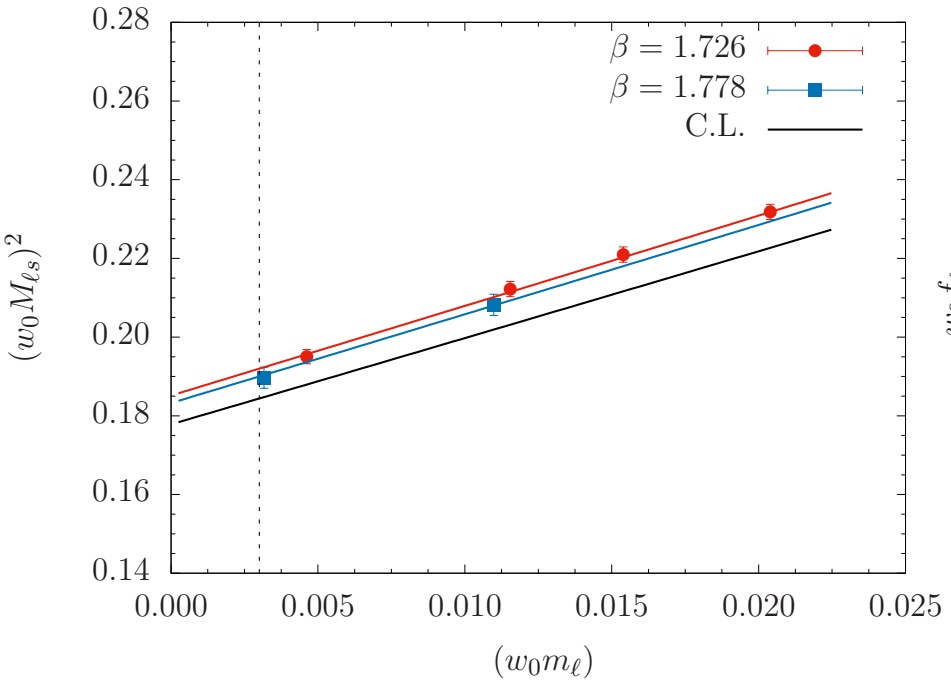

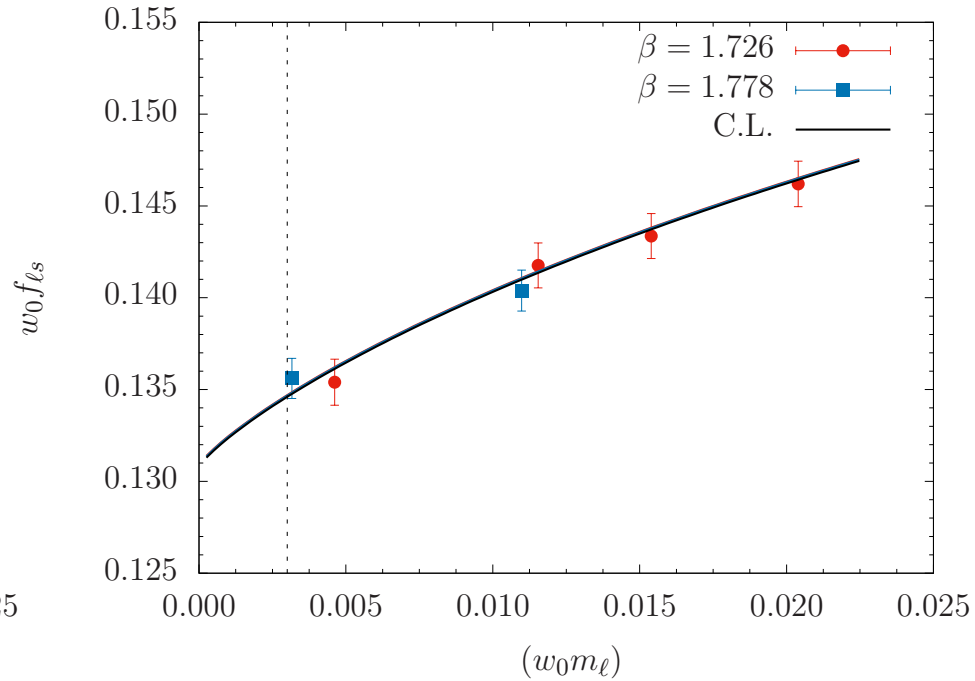

$m_s(\overline{\text{MS}}, 2\text{GeV}) = 96.5(6.2)$ MeV;

$\chi^2/\text{d.o.f.} = 0.11.$

$f_\text{K} = 155.0(2.2)$ MeV;

$\chi^2/\text{d.o.f.} = 0.54.$

Strange sector - 3

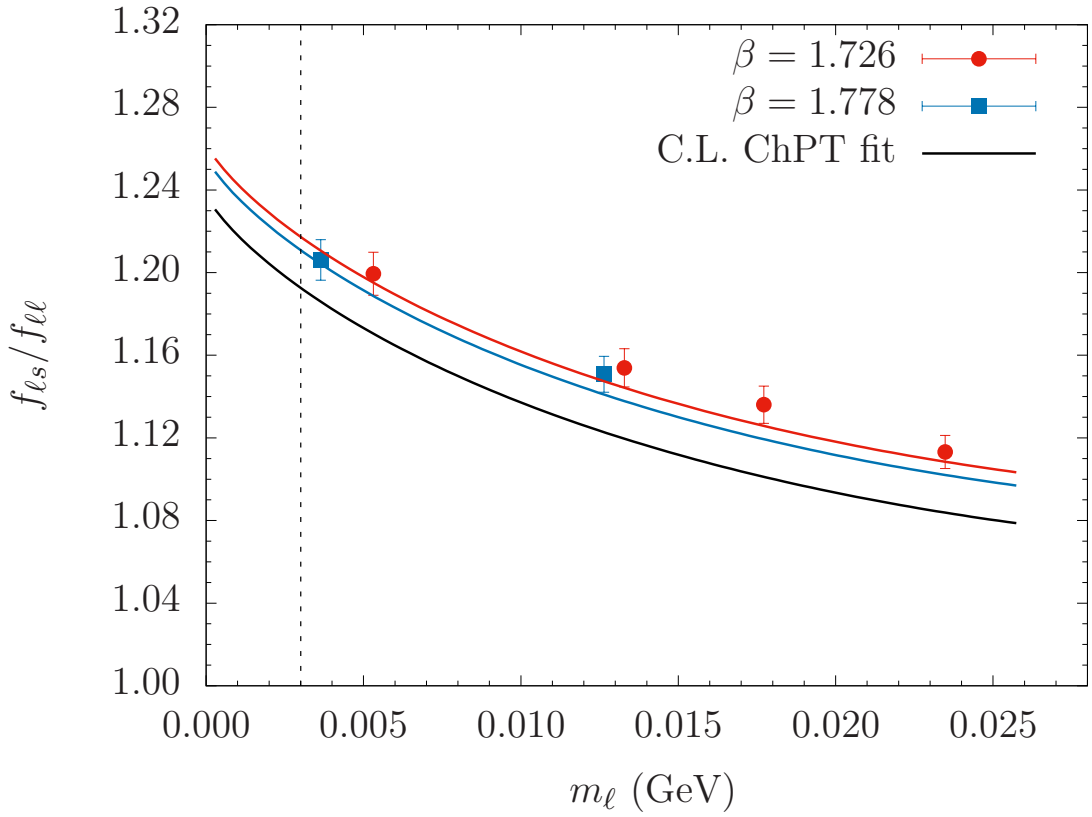

$f_K/f_\pi = 1.192(12)$; $\chi^2/\text{d.o.f.} = 0.12$.

Charm sector - 1

- Fit ansätze:

(see ETMC arXiv:1403.4504 & arXiv:1411.7908)

1. $M_{\ell c} = P_0 + P_1 m_\ell + (P_2 m_\ell^2) + P_3 (a/w_0)^2$
2. $M_{sc} = P_0' + P_1' m_\ell + (P_2' m_\ell^2) + P_3' (a/w_0)^2$

3a. $f_{sc} = \hat{P}_0{}' + \hat{P}_1{}' m_\ell + (\hat{P}_2{}' m_\ell^2) + \hat{P}_3{}' (a/w_0)^2$

3b. $(f_{sc}/M_{sc}) M_{Ds}^{expt.} = \hat{P}_0 + \hat{P}_1 m_\ell + (\hat{P}_2 m_\ell^2) + \hat{P}_3 (a/w_0)^2$

4a. $(f_{sc}/f_{\ell c})/(f_{\ell s}/f_{\ell \ell}) = \tilde{P}_0 \left(1 + [(9/4\hat{g}^2 - 1/2)\, \xi log \xi] + \tilde{P}_1 m_\ell + \tilde{P}_3 (a/w_0)^2\right)$

4a. $(f_{sc}/f_{\ell c}) = \tilde{P}_0' + \tilde{P}_1' m_\ell + \tilde{P}_3' (a/w_0)^2$

- use correlation functions $C_{PP}(t)$ (Smeared-Local & Smeared-Smeared).
- $m_c = \mu_c / Z_P$.
- $af_{\rm PS} = (a\mu_{\ell,s} + a\mu_c) \dfrac{|g_{\rm PS}|}{aM_{\rm PS} \sinh(aM_{\rm PS})}$

Charm sector - 2

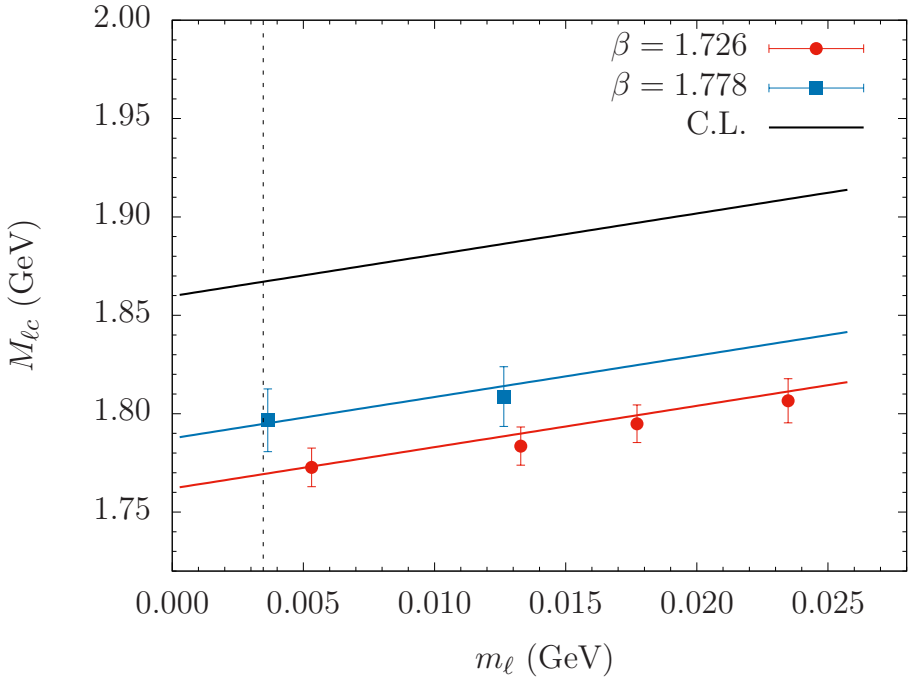

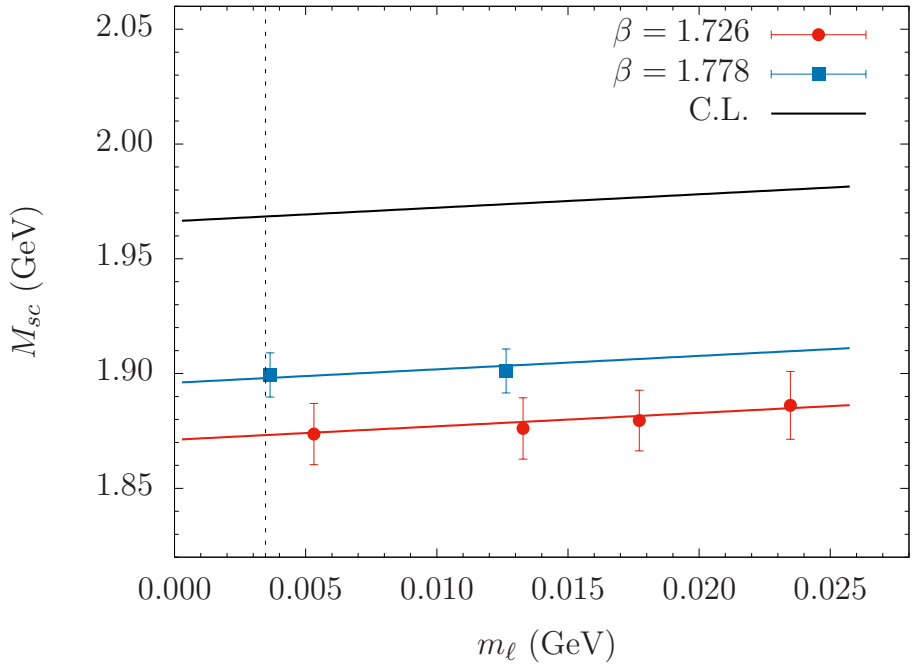

fit ansatz 1.:

$m_c(\overline{\text{MS}}, 2\text{GeV}) = 1.105(61)$ MeV;

$\chi^2/\text{d.o.f.} = 0.05$.

fit ansatz 2.:

$m_c(\overline{\text{MS}}, 2\text{GeV}) = 1.112(55)$ MeV;

$\chi^2/\text{d.o.f.} = 0.04$.

- m_c estimates employing either $M_{\ell c}$ or M_{sc} data (and the corresponding experimental values for M_D and M_{D_s}) are compatible within a small fraction of the standard deviation.

Charm sector - 3

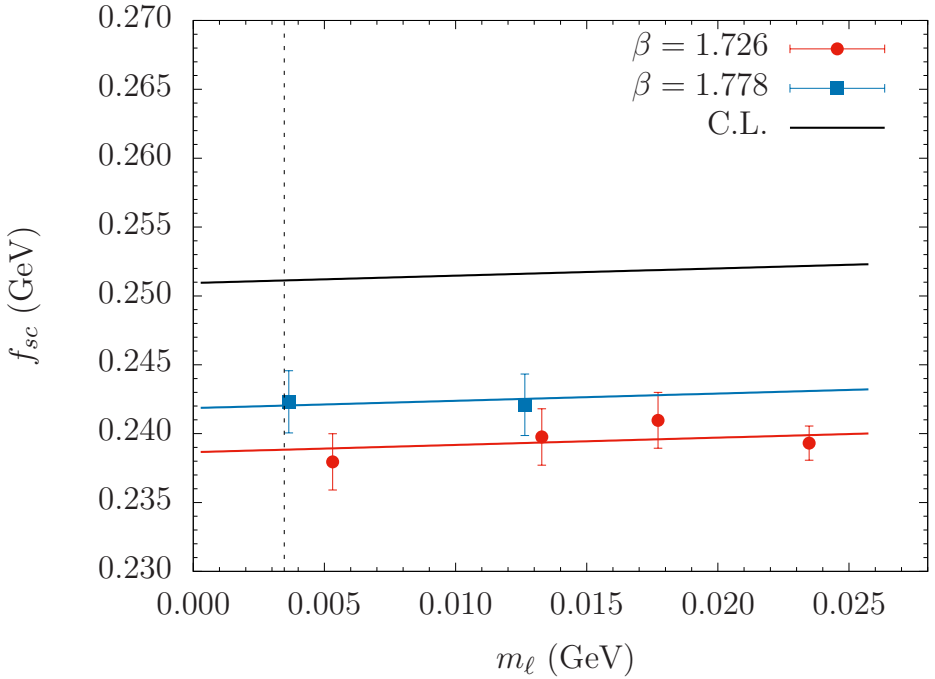

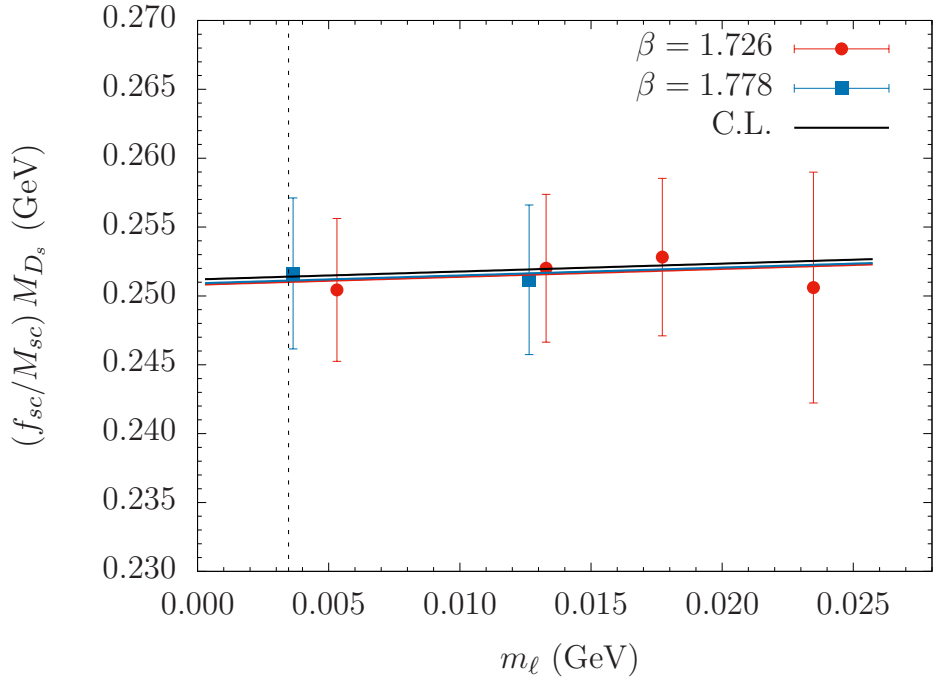

fit ansatz 3a.:

$f_{Ds} = 251(5)$ MeV;

$\chi^2/\text{d.o.f.} = 0.32$.

fit ansatz 3b.:

$f_{Ds} = 251(5)$ MeV;

$\chi^2/\text{d.o.f.} = 0.04$.

- f_{Ds} results from both methods show nice agreement, though cutoff effects are different.

Charm sector - 4

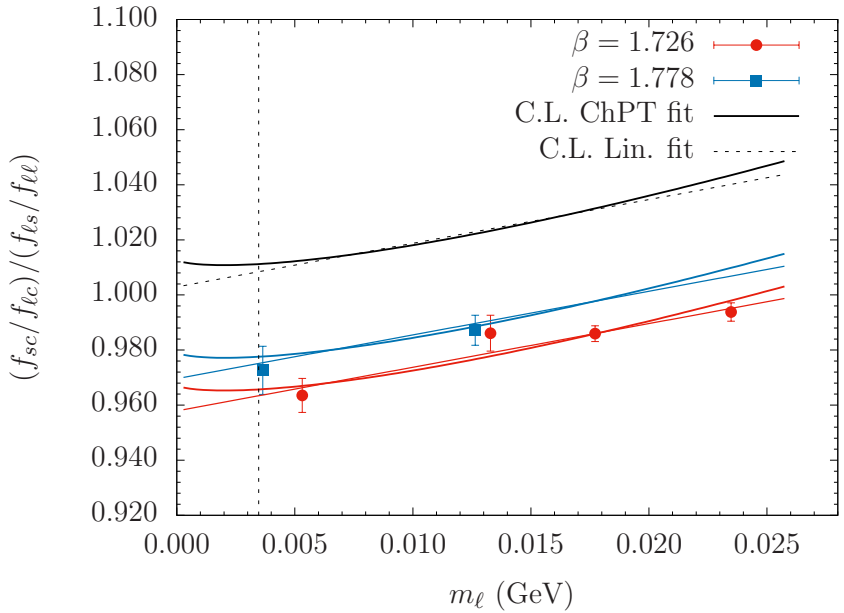

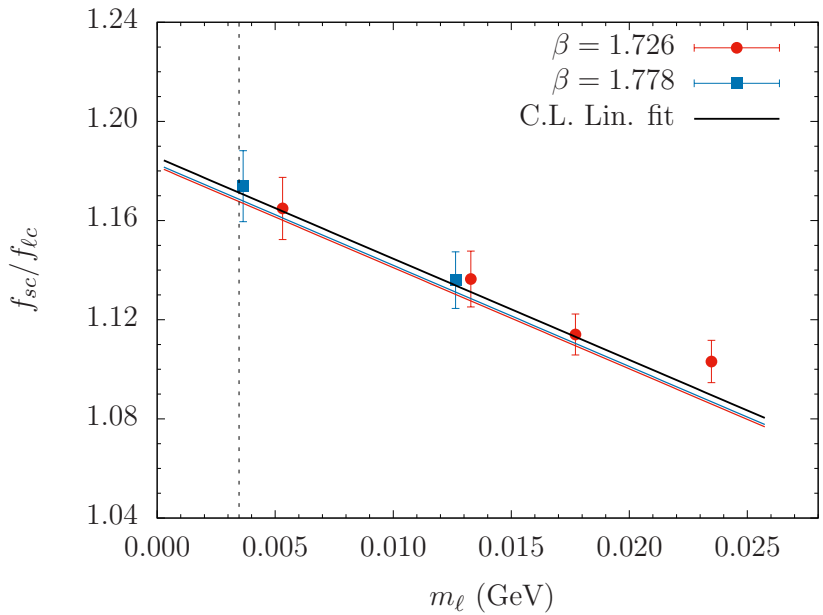

fit ansatz 4a.:

$f_{Ds}/f_D = 1.193(24)$;

$\chi^2/\text{d.o.f.} = 0.82\,\&\,0.74$

(ChPT & Lin. fit).

$f_D = f_{Ds}/(f_{Ds}/f_D) = 210(5)$ MeV.

fit ansatz 4b.:

$f_{Ds}/f_D = 1.173(25)$;

$\chi^2/\text{d.o.f.} = 0.27$.

$f_D = f_{Ds}/(f_{Ds}/f_D) = 214(5)$ MeV;

$f_D(\text{direct comp.}) = 213(4)$ MeV;

- f_{Ds}/f_D results from both methods are in good agreement within errors, though cutoff effects and values for the slope wrt m_ℓ appear quite different. As for the impact of the NLO (HM)ChPT term in fitting

Comments

- This *preliminary* analysis, employing data from only two lattice spacings, leads to results for the quark masses and decay constants in the Light, Strange and Charm sectors that are in good agreement with the corresponding FLAG19 values, though our errors are still quite large.

- Setting the scale from f_π we get w_0 compatible within 1σ with the coresponding MILC determination.

- Total uncertainties are expected to be drastically reduced when the datapoints from B.14.64 and in particular from C.060.80, refering to the finest lattice spacing at the physical pion mass, will be included in our analysis.

- The difference (at the level of $1\sigma \sim 6\%$) for the u/d quark mass estimates obtained with Z_P from M1 and M2 seems to be much reduced when data from the finest lattice spacing are included (using a reasonable guess for the value of the corresponding values of Z_P).

cC211.06.80	a mu_s= 0.0128		a mu_s= 0.0161		a mu_s= 0.0183	
	am	chi^2	am	chi^2	am	chi^2
2 state	0.550(8)	1.11	0.577(7)	1.23	0.604(6)	1.33
Plateau	0.551(7)	1.4	0.576(7)	1.67	0.606(7)	1.84

cB211.072.64	a mu_s= 0.0148		a mu_s= 0.0185		a mu_s= 0.0222	
	am	chi^2	am	chi^2	am	chi^2
2 state	0.680(5)	0.56	0.700(6)	0.57	0.719(3)	0.61
Plateau	0.682(5)	0.61	0.701(5)	0.63	0.720(4)	0.68

cA211.12.48	a mu_s= 0.0182		a mu_s= 0.0227		a mu_s= 0.0273	
	am	chi^2	am	chi^2	am	chi^2
2 state	0.784(5)	1.18	0.816(5)	1.1	0.851(4)	0.95
Plateau	0.786(4)	1.09	0.818(7)	0.8	0.853(6)	0.65

cB211.25.48	a mu_s= 0.0148		a mu_s= 0.0185		a mu_s= 0.0222	
	am	chi^2	am	chi^2	am	chi^2
2 state	0.664(7)	1.44	0.700(4)	1.95	0.721(5)	1.59
Plateau	0.663(6)	1.77	0.700(4)	2.65	0.724(4)	2.24

cA211.30.32	a mu_s= 0.0182		a mu_s= 0.0227		a mu_s= 0.0273	
	am	chi^2	am	chi^2	am	chi^2
2 state	0.802(11)	1.27	0.837(4)	1.76	0.870(4)	1.78
Plateau	0.804(5)	1.05	0.838(3)	1.26	0.871(3)	1.32

cA211.40.24	a mu_s= 0.0182		a mu_s= 0.0227		a mu_s= 0.0273	
	am	chi^2	am	chi^2	am	chi^2
2 state	0.819(9)	1.12	0.851(8)	1.8	0.882(7)	1.15
Plateau	0.821(6)	1.12	0.853(5)	1.16	0.884(5)	1.28

cA211.53.24	a mu_s= 0.0182		a mu_s= 0.0227		a mu_s= 0.0273	
	am	chi^2	am	chi^2	am	chi^2
2 state	0.807(9)	0.82	0.842(7)	0.85	0.876(7)	0.89
Plateau	0.806(9)	0.79	0.576(7)	0.86	0.877(6)	0.92

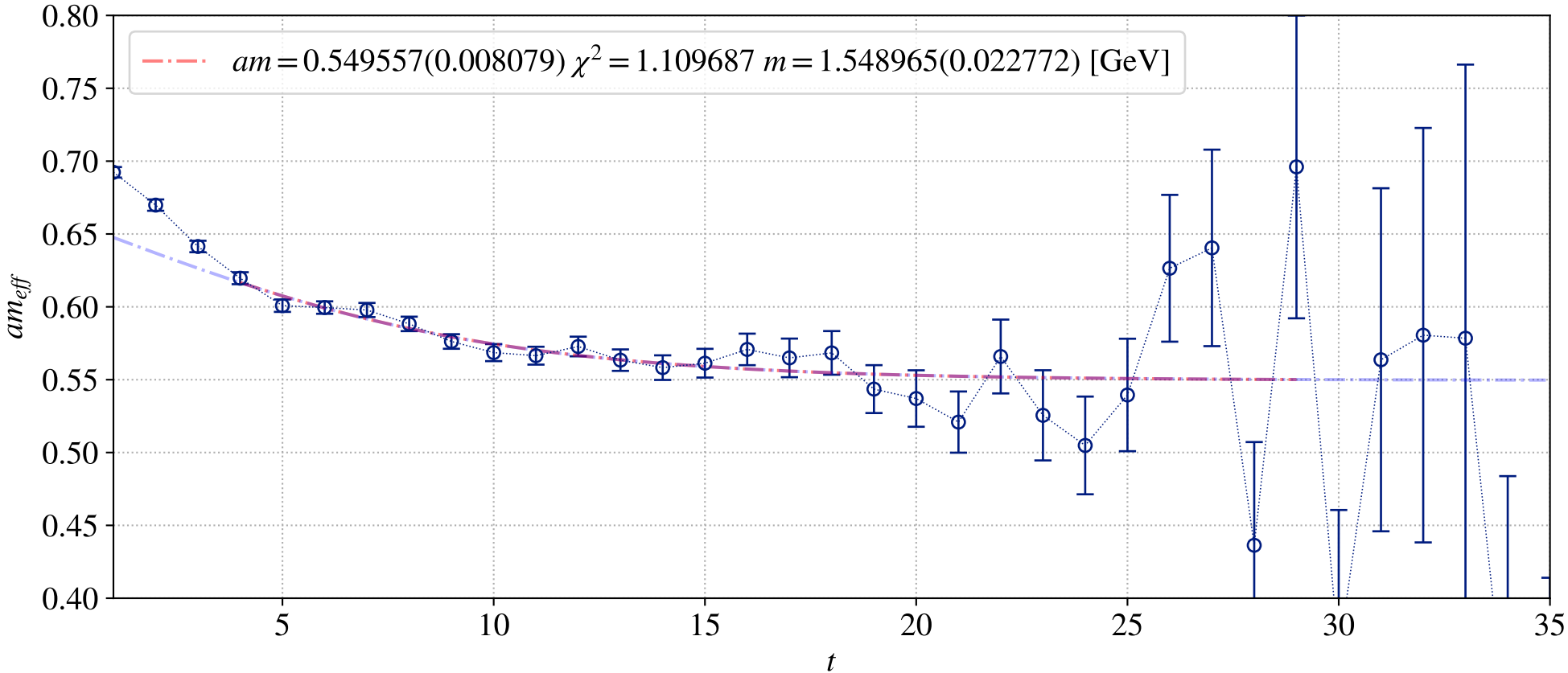
$am = 0.549557(0.008079)\ \chi^2 = 1.109687\ m = 1.548965(0.022772)$ [GeV]
am_{eff}
t
0.80
0.75
0.70
0.65
0.60
0.55
0.50
0.45
0.40
5
10
15
20
25
30
35

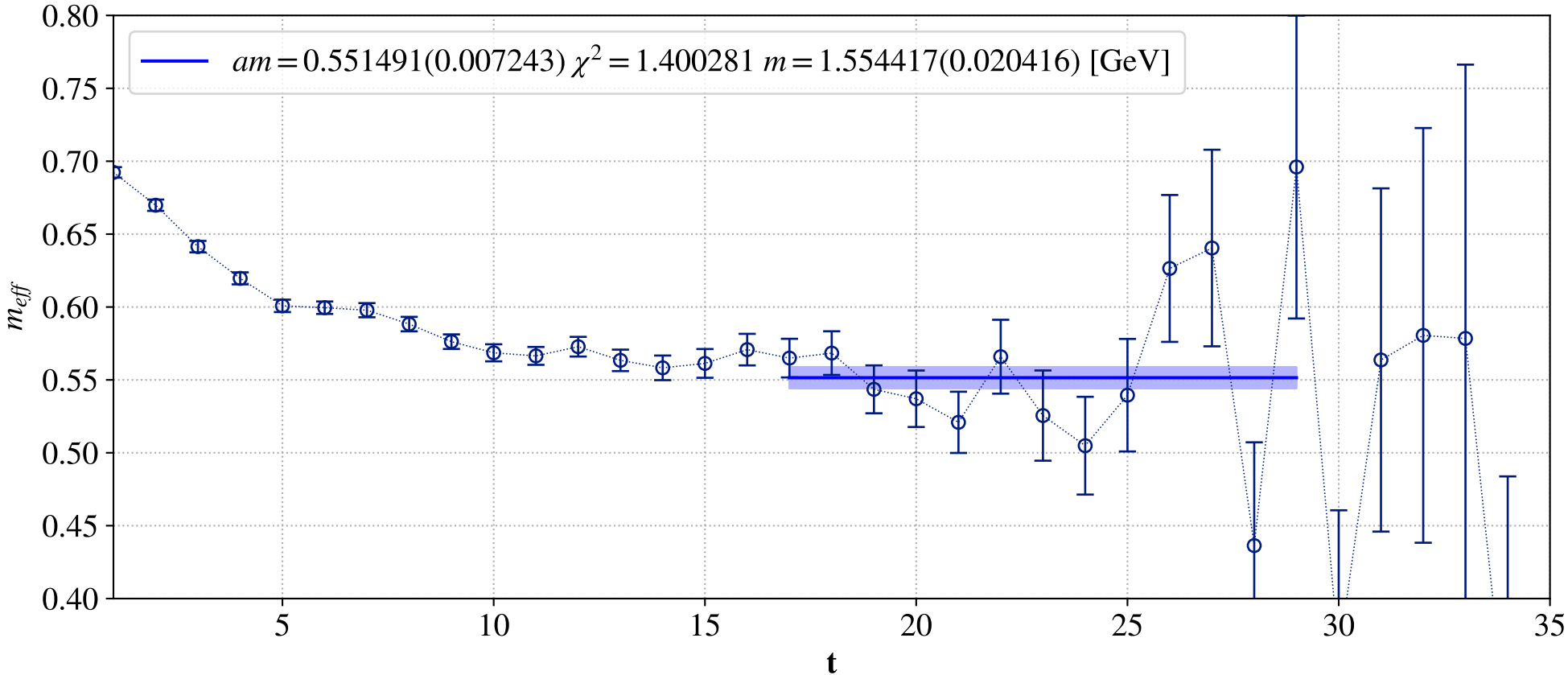
$am = 0.551491(0.007243)\ \chi^2 = 1.400281\ m = 1.554417(0.020416)$ [GeV]
m_{eff}
t
0.80
0.75
0.70
0.65
0.60
0.55
0.50
0.45
0.40
5
10
15
20
25
30
35

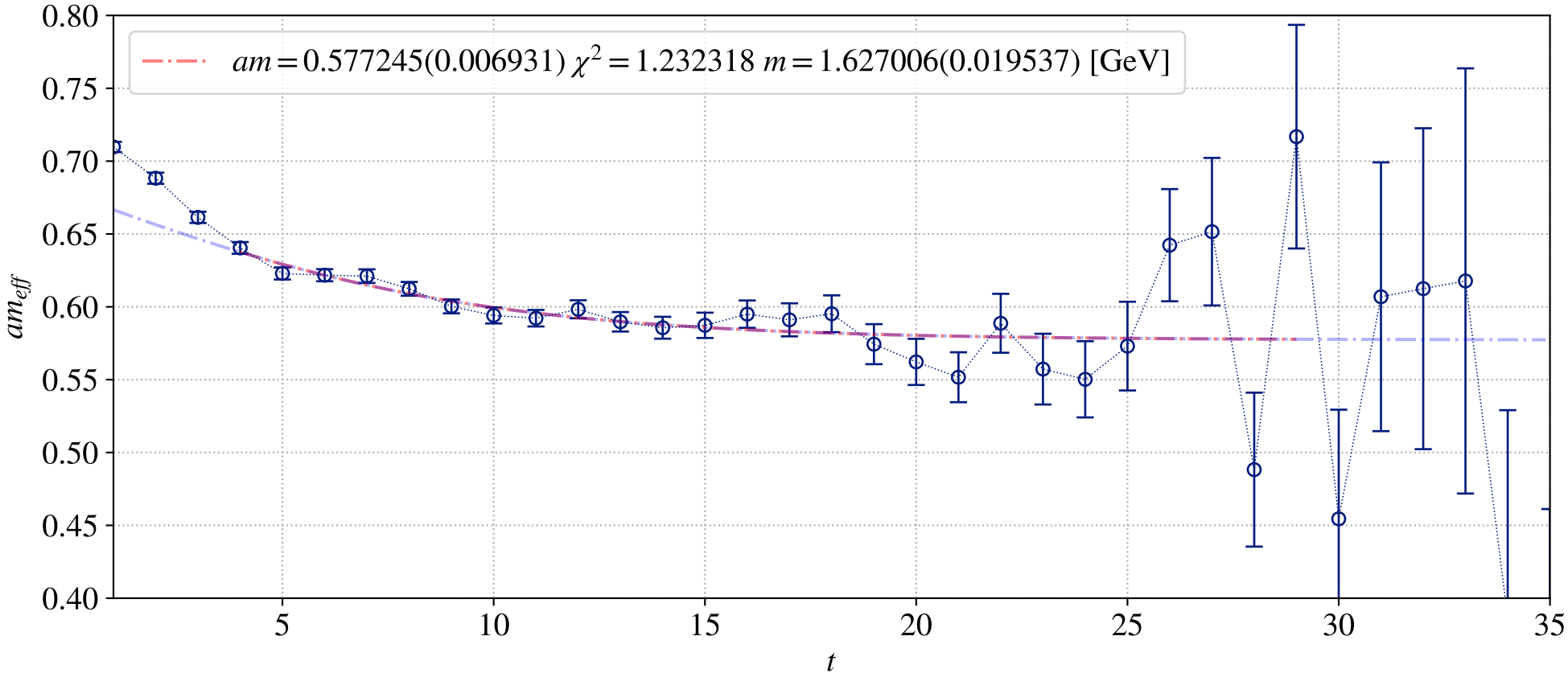
$am = 0.577245(0.006931)\ \chi^2 = 1.232318\ m = 1.627006(0.019537)$ [GeV]
am_{eff}
t
0.80
0.75
0.70
0.65
0.60
0.55
0.50
0.45
0.40
5
10
15
20
25
30
35

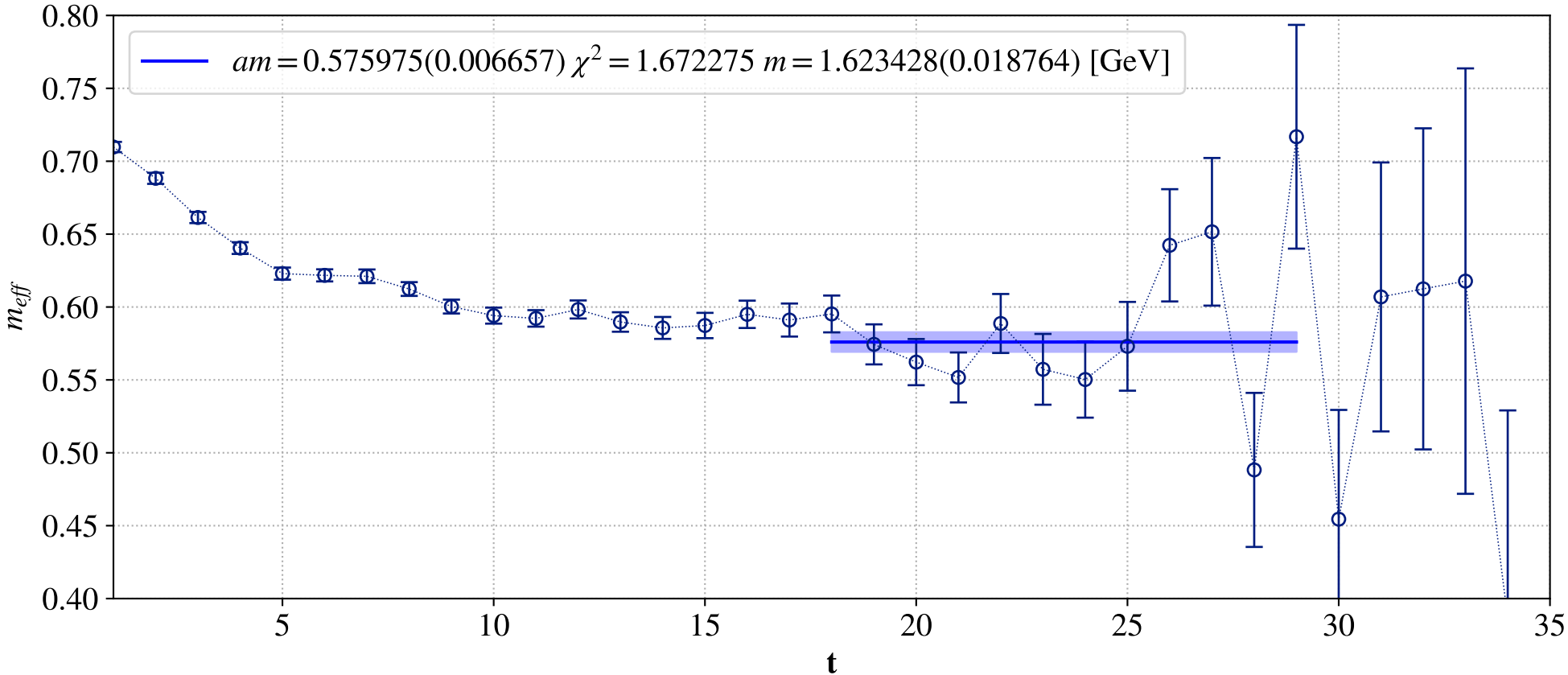
$am = 0.575975(0.006657)\ \chi^2 = 1.672275\ m = 1.623428(0.018764)$ [GeV]
m_{eff}
t
0.80
0.75
0.70
0.65
0.60
0.55
0.50
0.45
0.40
5
10
15
20
25
30
35

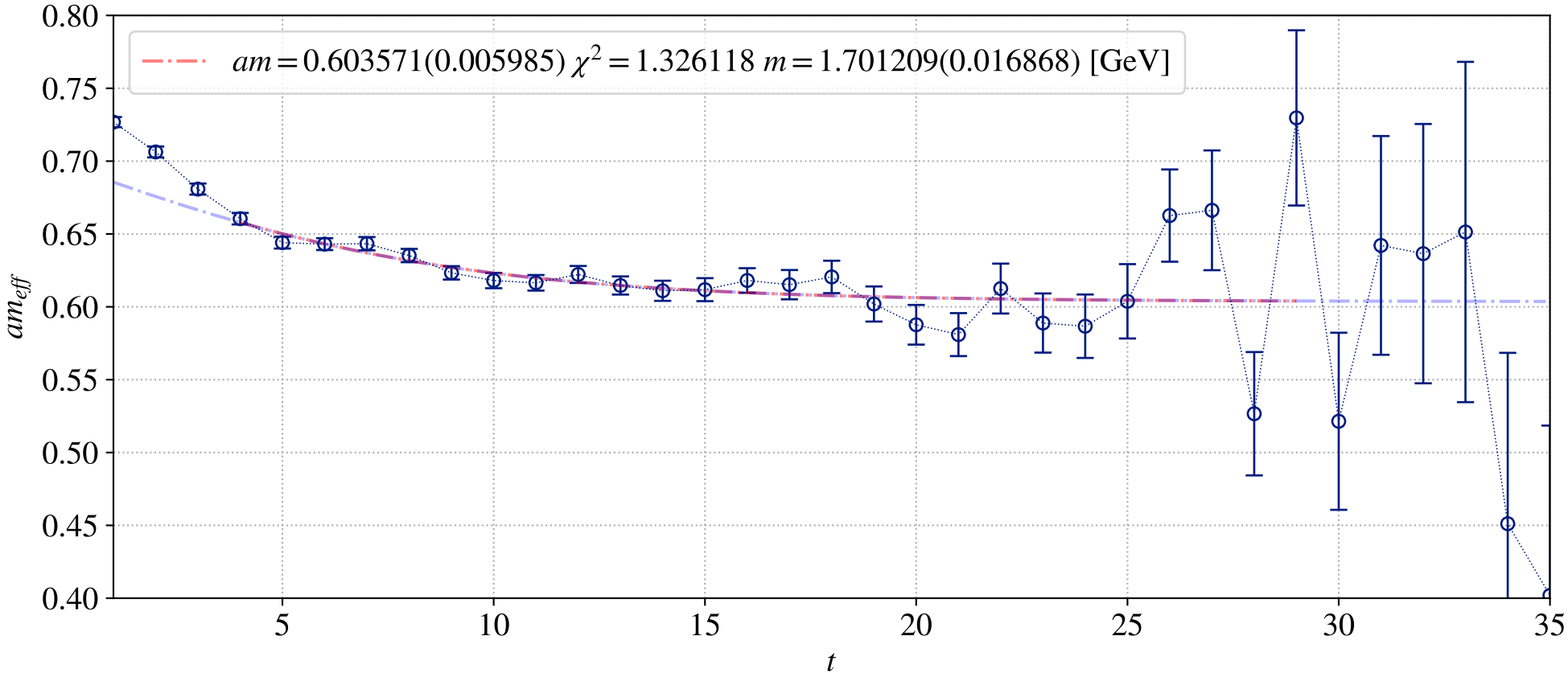
$am = 0.603571(0.005985)\ \chi^2 = 1.326118\ m = 1.701209(0.016868)$ [GeV]
0.80
0.75
0.70
0.65
0.60
0.55
0.50
0.45
0.40
am_{eff}
5
10
15
20
25
30
35
t

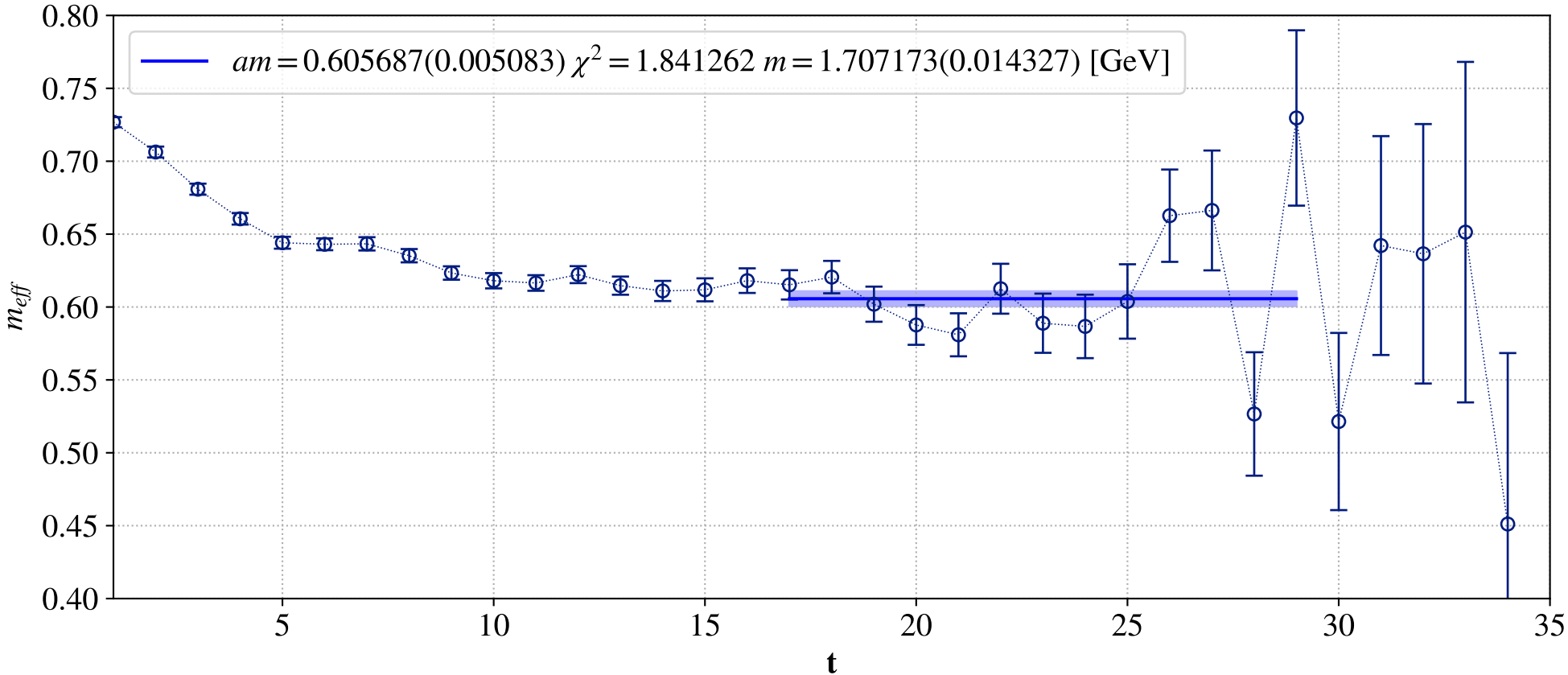
$am = 0.605687(0.005083)\ \chi^2 = 1.841262\ m = 1.707173(0.014327)$ [GeV]
m_{eff}
t
0.80
0.75
0.70
0.65
0.60
0.55
0.50
0.45
0.40
5
10
15
20
25
30
35

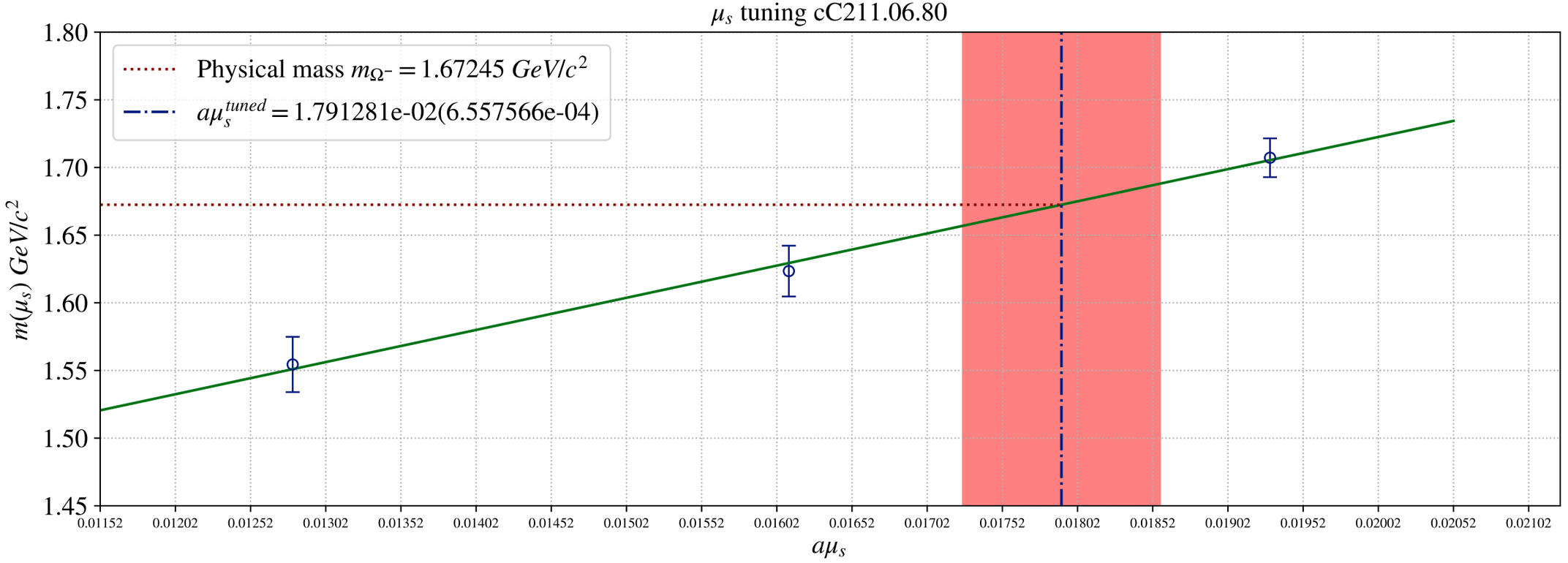
μ_s tuning cC211.06.80
Physical mass $m_{\Omega^-} = 1.67245\ GeV/c^2$
$a\mu_s^{tuned} = 1.791281\text{e-}02(6.557566\text{e-}04)$
$m(\mu_s)\ GeV/c^2$
1.80
1.75
1.70
1.65
1.60
1.55
1.50
1.45
0.01152
0.01202
0.01252
0.01302
0.01352
0.01402
0.01452
0.01502
0.01552
0.01602
0.01652
0.01702
0.01752
0.01802
0.01852
0.01902
0.01952
0.02002
0.02052
0.02102
$a\mu_s$

Note on the determination of w_0 from an SU(2) ChPT analysis of f_π

by Silvano

July 17, 2019

1 The pion decay constant f_π within SU(2) ChPT

In this note we consider the pion decay constant calculated adopting the ETMC ensembles with $N_f = 2+1+1$ Wilson Clover twisted-mass fermions, which include the physical pion point. We will denote by $m_\ell = m_u = m_d$ the sea light-quark mass in isoQCD.

Within SU(2) Chiral Perturbation Theory (SU(2) ChPT) the pion decay constant f_π is given at next-to-leading-order (NLO) by

$$f_\pi = f\left[1 - 2\xi_\ell \log(\xi_\ell) + 2A_1\xi_\ell\right] \ , \tag{1}$$

where

$$\xi_\ell \equiv \frac{2B\, m_\ell}{(4\pi f)^2} \ , \tag{2}$$

while B and f are the LO SU(2) ChPT low-energy constants (LECs) and the NLO LEC A_1 is evaluated at a ChPT renormalization scale μ equal to $\mu = 4\pi f$. The change of the NLO LEC with respect to a variation of the scale μ is governed by the corresponding anomalous dimensions. Using the physical pion mass M_π^{phys} as the standard reference value, one has

$$\bar{\ell}_4 = A_1 + 2\log\left(\frac{4\pi f}{M_\pi^{phys}}\right) \ . \tag{3}$$

2 Finite volume effects within NLO SU(2) ChPT

The structure of finite volume effects (FVEs) can be studied using ChPT. At NLO FVEs come entirely from the discretized sum over periodic momenta of the loop contributions. For a finite spatial volume $V = L^3$ one has

$$f_\pi(L) = f\left[1 - 2\xi_\ell \log(\xi_\ell) + 2A_1\xi_\ell + \Delta^\pi_{FVE}(L)\right] \ . \tag{4}$$

The correction term $\Delta^{\pi}_{FVE}(L)$ can be obtained from the chiral log via the following replacement (see Appendix C of Ref. [1])

$$\xi_\ell \log(\xi_\ell) \to \frac{\xi_\ell}{2}\, \widetilde{g}_1(\lambda) \ , \tag{5}$$

where $\lambda \equiv \sqrt{2Bm_\ell}L = \sqrt{\xi_\ell}\ 4\pi f L$ and

$$\widetilde{g}_1(\lambda) = 4\sum_{n=1}^{\infty} \frac{m(n)}{\sqrt{n}\lambda} K_1\left(\sqrt{n}\lambda\right) \tag{6}$$

with K_1 being a Bessel function of the second kind and $m(n)$ the multiplicities of a three-dimensional vector $\vec{n}$ having integer norm n (i.e. $m(n) = \{6, 12, 8, 6, ...\}$). At sufficiently large values of λ the Bessel function can be replaced by its asymptotic expansion, which leads to

$$\widetilde{g}_1(\lambda) \simeq 4\sqrt{\frac{\pi}{2}} \sum_{n=1}^{\infty} \frac{m(n)}{(\sqrt{n}\lambda)^{3/2}} e^{-\sqrt{n}\lambda} \ . \tag{7}$$

Thus, one has

$$\Delta^{\pi}_{FVE}(L) = -\xi_\ell \widetilde{g}_1(\lambda) \ . \tag{8}$$

3 ETMC ensembles

Some simulation details of the ETMC ensembles considered in this note are collected in Table 1, where the values for the gradient-flow scale in lattice units, w_0/a, come from Ref. [2]. As described in Ref. [3], the twisted-mass fermion formulation was employed including a Clover term, which helps in reducing cutoff and isospin breaking effects. The Wilson mass of the two degenerate light-quarks is chosen in order to guarantee automatic $\mathcal{O}(a)$-improvement, while the twisted masses of the heavier strange and charm quarks are tuned to their physical values [3].

In what follows we will use for the physical pion mass in isoQCD the value recommended by FLAG-3 [4], namely

$$M_\pi^{phys} = M_\pi^{isoQCD} = 134.8\ (3)\ \text{MeV} \ . \tag{9}$$

Note that for the ensembles cB07.64 and cC06.80, corresponding respectively to a lattice spacing equal to $a \simeq 0.079$ and $a \simeq 0.068$ fm, the pion masses are simulated quite close to the FLAG-3 value (9).

For each ensemble we compute the 2-point pion correlator given by

$$C(t) = \frac{1}{L^3} \sum_{x,z} \langle 0 |\, P_5(x) P_5^\dagger(z)\, | 0 \rangle\, \delta_{t,(t_x - t_z)} \ , \tag{10}$$

ensemble	β	V/a^4	w_0/a	$a\mu_\ell$	M_π (MeV)	L (fm)	$M_\pi L$
cA40.24	1.726	$24^3 \times 48$	1.8347(52)	0.00400	309.7(2.2)	2.21	3.47
cA53.24		$24^3 \times 48$		0.00530	355.7(1.7)	2.21	3.99
cA30.32		$32^3 \times 64$		0.00300	270.4(0.9)	2.95	4.04
cA12.48		$48^3 \times 96$		0.00120	170.7(0.6)	4.43	3.83
cB25.48	1.778	$48^3 \times 96$	2.1331(47)	0.00250	260.4(1.3)	3.81	5.03
cB07.64		$64^3 \times 128$		0.00072	141.4(0.7)	5.08	3.64
cC06.80	1.836	$80^3 \times 160$	2.4988(34)	0.00060	137.7(0.5)	5.42	3.78

Table 1: *Summary of the simulated light-quark sea bare mass, $a\mu_\ell$, of the πmeson mass, of the lattice size L and of the product $M_\pi L$ for the various ETMC gauge ensembles used in this note. In the fourth column the values estimated by ETMC [2] for the gradient-flow scale in lattice units, w_0/a, are shown. In the sixth and seventh columns the values of M_π and L correspond to an absolute scale w_0 equal to $w_0 = 0.16923(38)$ fm (see next Section).*

where $P_5(x) = \overline{q}_\ell(x)\gamma_5 q_\ell(x)$ is a local interpolating pion field. The Wilson parameters of the two mass-degenerate valence quarks are always chosen to have opposite values. In this way the squared pion mass differs from its continuum counterpart only by terms of $\mathcal{O}(a^2\mu_\ell)$ [5, 6].

At large time distances one has

$$C(t) \xrightarrow[t \gg a,\ (T-t) \gg a]{} \frac{\mathcal{Z}_\pi}{2M_\pi} \left[e^{-M_\pi t} + e^{-M_\pi (T-t)}\right] \ , \tag{11}$$

so that the pion mass M_π and the matrix element $\mathcal{Z}_\pi = |\langle \pi | \overline{q}_\ell \gamma_5 q_\ell | 0 \rangle|^2$ can be extracted from the exponential fit given in the r.h.s. of Eq. (11). The time intervals $[t_{min}, t_{max}]$ adopted for the fit (11) of the pion correlation function (10) are collected in Table 2.

For maximally twisted fermions the value of $\mathcal{Z}_\pi$ determines the pion decay constant f_π without the need of the knowledge of any renormalization constant [7, 5], namely

$$a f_\pi = 2a\mu_\ell \frac{\sqrt{a^4 \mathcal{Z}_\pi}}{aM_\pi \sinh(aM_\pi)} \ . \tag{12}$$

In the case of the ensemble cA211.12.48 a correction due to a deviation from maximal twist should be applied. We use the following approximate formula

$$f_\pi|_{corrected} \simeq f_\pi \cdot K_\ell \ , \tag{13}$$

where

$$K_\ell \equiv \sqrt{1 + (Z_A \ \mu_{PCAC}/\mu_\ell)^2} \ , \tag{14}$$

ensemble	β	V/a^4	$[t_{\min}/a,\, t_{\max}/a]$
cA40.24	1.726	$24^3 \times 48$	[13, 22]
cA53.24		$24^3 \times 48$	[13, 22]
cA30.32		$32^3 \times 64$	[13, 28]
cA12.48		$48^3 \times 96$	[13, 40]
cB25.48	1.778	$48^3 \times 96$	[14, 40]
cB07.64		$64^3 \times 128$	[14, 56]
cC06.80	1.836	$80^3 \times 160$	[15, 70]

Table 2: *The time intervals $[t_{min}, t_{max}]$ adopted for the fit (11) of the PS-PS correlation functions.*

μ_{PCAC} is the bare PCAC mass, Z_A is the renormalization constant of the axial current and μ_ℓ is the bare twisted mass of the light valence quarks. For the squared pion mass the analogous correction is given by

$$M_\pi^2|_{corrected} = M_\pi^2/K_\ell \ . \tag{15}$$

For the ensemble cA211.12.48 one has $Z_A \simeq 0.75$ and $\mu_{PCAC}/\mu_\ell \simeq -0.21$ (5) [8]. Note that, because of the approximation (13) one has $M_\pi^2 f_\pi|_{corrected} \simeq M_\pi^2 f_\pi$.

The statistical accuracy of the correlator (10) is significantly improved by using the so-called "one-end" stochastic method [9], which includes spatial stochastic sources at a single time slice chosen randomly. Statistical errors on the pion mass and decay constant are evaluated using the jackknife procedure.

In Fig. 1 we show the results for the pion decay constant f_π assuming $w_0 = 0.16923(38)$ fm (see next Section). Note that the errors of the data (statistical + scale setting) lie in the range $0.4 \div 0.8\%$.

4 SU(2) ChPT analysis of f_π

Let's now apply the SU(2) ChPT predictions for interpolating the pion data to the physical pion mass and to extrapolate them to the continuum and infinite volume limits.

First of all we re-express the quantity ξ_ℓ (see Eq. (2)) in terms of the pion mass

$$\xi_\ell \to \xi \equiv \frac{M_\pi^2}{(4\pi f)^2} = \frac{(w_0 M_\pi)^2}{(4\pi w_0 f)^2} \ , \tag{16}$$

where only the knowledge of w_0/a is required to calculate $w_0 M_\pi$ and the free parameter becomes $w_0 f$.

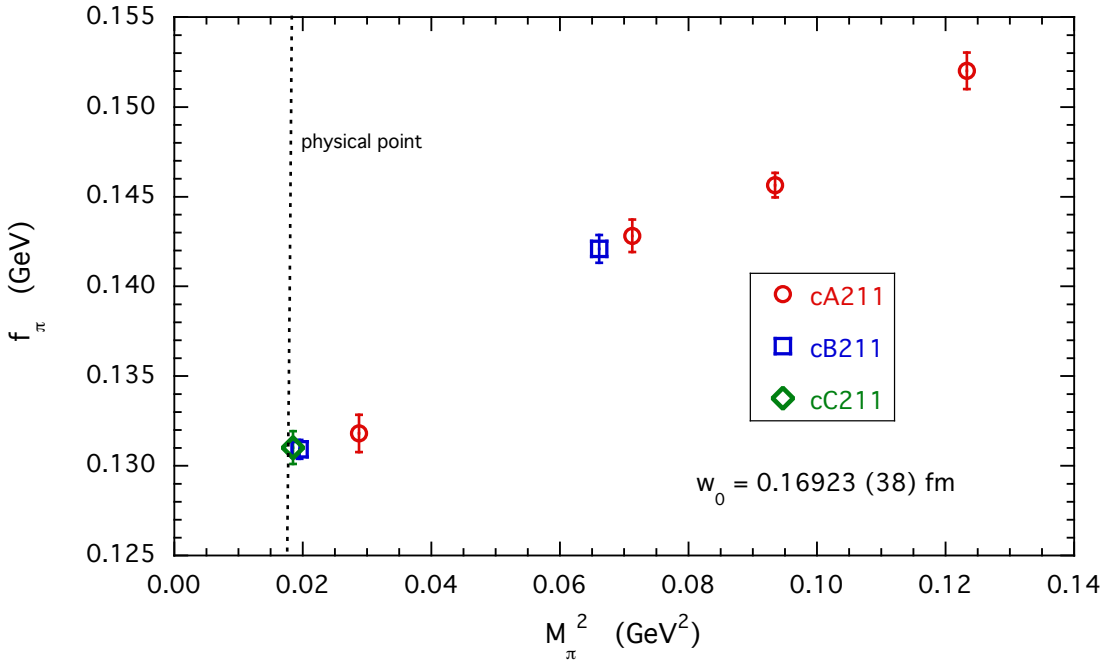

Figure 1: *Values of the pion decay constant f_π. The vertical dotted line indicates the location of the physical pion point $(M_\pi^{phys})^2 = 0.0182$ GeV^2. The physical units are obtained assuming $w_0 = 0.16923(38)$ fm (see next Section).*

Then we add to Eq. (4) a term quadratic in the light-quark mass (i.e., quartic in the pion mass) as well as a discretization effect, namely

$$f_\pi = f\left[1 - 2\xi\log(\xi) + 2A_1\xi + A_2\xi^2 + \frac{a^2}{w_0^2}D_0 + \Delta^\pi_{FVE}(L)\right] \tag{17}$$

with $\Delta^\pi_{FVE}(L) = -\xi\widetilde{g}_1(\lambda)$ and $\lambda = \sqrt{\xi}4\pi f L$.

Obviously we do not fit the data for f_π, which would require the knowledge of w_0. Instead we construct the ratio

$$\xi_\pi \equiv \frac{M_\pi^2}{(4\pi f_\pi)^2}\ , \tag{18}$$

which does not depend at all on w_0 and on w_0/a. The fitting function is now given by

$$\xi_\pi = \frac{\xi}{\left[1 - 2\xi\log(\xi) + 2A_1\xi + A_2\xi^2 + \frac{a^2}{w_0^2}D_0 + \Delta^\pi_{FVE}(L)\right]^2}\ , \tag{19}$$

where the denominator is left as it is. The free parameters appearing in Eq. (19) are: A_1, A_2, D_0 and $w_0 f$. After the fitting procedure is carried out, the physical

value of the variable ξ can be inferred from the fit using the physical value of ξ_π. For the latter we make use of physical pion mass (9) and of the value $f_\pi^{phys} = 130.4(2)$ MeV adopted by ETMC in Ref. [10] and based on the value of the CKM entry $|V_{ud}|$ from Ref. [11]. Consequently, from the physical value of ξ and the value of $w_0 f$ obtained from the fitting procedure we get the value of $w_0 M_\pi^{phys}$ and, therefore, the one of w_0.

We start by considering the NLO fit, i.e. $A_2 = 0$. This fits works quite well. The FVEs are successfully taken into account using the NLO SU(2) ChPT prediction $\Delta_{FVE}^{\pi}(L)$, while the discretization term can be safely put to zero (i.e. $D_0 = 0$). The resulting χ^2/(d.o.f.) is good: χ^2/(d.o.f.) $\simeq 0.8$ for 7 data points and 2 parameters. Following the procedure previously explained, we get

$$w_0 = 0.16899\ (32)\ \text{fm} \tag{20}$$

with $f = 122.5\ (0.4)$ MeV and $\bar{\ell}_4 = 4.20(6)$ (see Eq. (3)).

The largest deviation occurs for the data point corresponding to the ensemble cA211.12.48, which receives corrections due to deviations from the maximal twist. Excluding the above data point, we obtain

$$w_0 = 0.16923\ (38)\ \text{fm} \tag{21}$$

with $f = 122.5\ (0.5)$ MeV and $\bar{\ell}_4 = 4.19(6)$. The corresponding χ^2/(d.o.f.) is now χ^2/(d.o.f.) $\simeq 0.6$ for 6 data points and 2 parameters. The nice quality of this fit is illustrated in Fig. 2. The only exception is the data point corresponding to the ensemble cA211.12.48. Therefore, in what follows the above data point will not be considered any more in the fitting procedures and we will refer to Eq. (21) as well as to the corresponding values of the LECs f and $\bar{\ell}_4$ as the NLO results.

Our finding (21) has a quite interesting relative error of $\simeq 0.2\%$. For comparison the recent MILC result [12] obtained at $N_f = 2 + 1 + 1$ is $w_0 = 0.1714(15)$ fm, which deviates from Eq. (21) only by $\simeq 1.4$ standard deviations thanks to the much larger uncertainty of the MILC result.

Concerning the LECS f and $\bar{\ell}_4$, the FLAG-4 estimates [13] at $N_f = 2+1+1$ are based on the ETMC results $f = 121.1(0.4)$ MeV and $\bar{\ell}_4 = 4.73(10)$ from Ref. [14]. In Ref. [10] a NLO fit applied to the ETMC data with $M_\pi < 300$ MeV yielded $f = 122.2(0.8)$ MeV and $\bar{\ell}_4 = 4.18(38)$.

Adding in the fitting procedure the quadratic term proportional to A_2 the quality of the fit improves significantly, χ^2/(d.o.f.) $\simeq 0.2$ (6 data points and 3 parameters), obtaining

$$w_0 = 0.16958\ (43)\ \text{fm} \tag{22}$$

with $f = 123.3\ (1.0)$ MeV and $\bar{\ell}_4 = 3.72(31)$. Thus, the above findings confirm the NLO results within larger uncertainties.

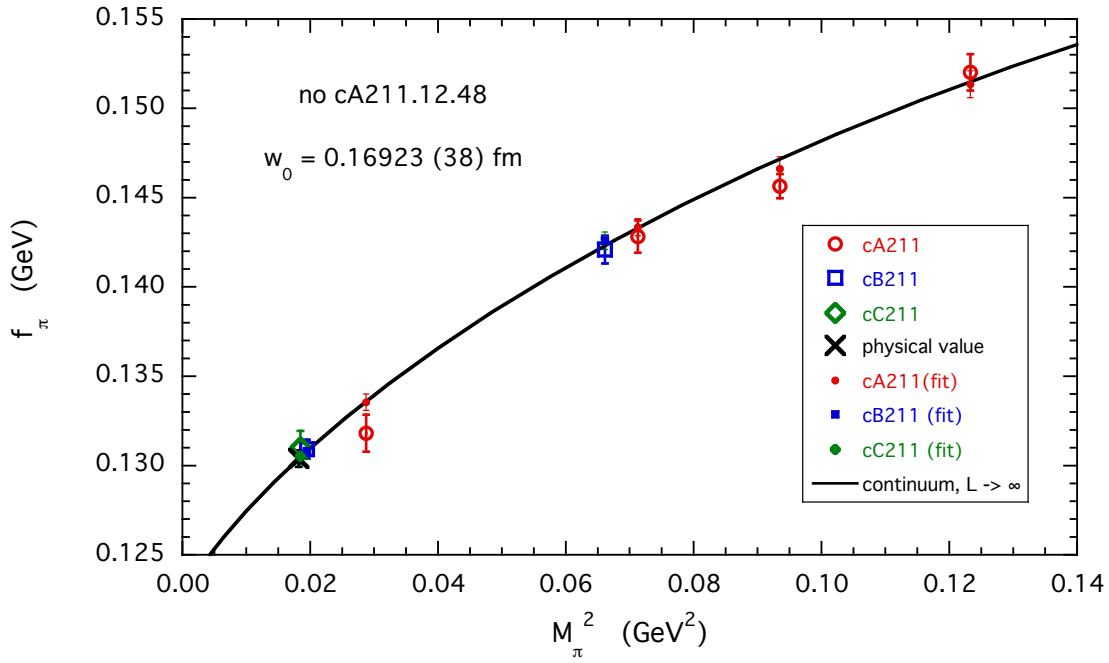

Figure 2: *The same data points as those in Fig. 1 (open markers) compared with the results of the NLO ChPT fit (17) with* $A_2 = D_0 = 0$ *(full dots) and excluding the data point corresponding to the ensemble cA211.12.48. The solid line represents the continuum and infinite volume limits of Eq. (17). The physical value of* f_π *corresponds to the value* $f_\pi^{phys} = 0.1304(2)$ *GeV adopted by ETMC in Ref. [10].*

For estimating the impact of FVEs we multiply the correction $\Delta_{FVE}(L)$ in Eq. (19) by a factor κ_{FVE}, which is then used as a free parameter in the fitting procedure. The factor κ_{FVE} turns out to be consistent with unity though within an almost 100% uncertainty, $\kappa_{FVE} = 2.0(1.9)$. We get

$$w_0 = 0.16940\ (38)\ \text{fm} \tag{23}$$

with $f = 122.4\ (0.5)$ MeV, $\bar{\ell}_4 = 4.23(13)$ and $\chi^2/(\text{d.o.f.}) \simeq 0.7$ (6 data points and 3 parameters). Again, the above findings confirm the NLO results.

We now add the discretization term proportional to D_0. The fitting procedure yields $D_0 = -0.086 \pm 0.107$, i.e. a value compatible with zero. Nevertheless its impact on the determination of w_0 is important, since we obtain

$$w_0 = 0.17247\ (37)\ \text{fm} \tag{24}$$

with $f = 122.3\ (0.3)$ MeV, $\bar{\ell}_4 = 4.28(19)$ and $\chi^2/(\text{d.o.f.}) \simeq 0.6$ (6 data points and 3 parameters). The result (24) differs from Eq. (21) by several standard deviations.

However, both are consistent with the MILC result $w_0 = 0.1714(15)$ fm [12] within the uncertainties.

In conclusion, the determination of w_0 from a SU(2) ChPT fit of the pion decay constant, evaluated using the ETMC ensembles with $N_f = 2+1+1$ Wilson Clover twisted-mass fermions, is in principle quite precise, see Eq. (21), but it suffers from a large uncertainty due to the possible presence of discretization effects. An interesting consistency with the MILC result $w_0 = 0.1714(15)$ fm [12] is observed within the uncertainties.

References

[1] G. Colangelo, S. Durr and C. Haefeli, Nucl. Phys. B **721** (2005) 136 doi:10.1016/j.nuclphysb.2005.05.015 [hep-lat/0503014].

[2] M. Garofalo et al., PRACE PLepNuGam project.

[3] C. Alexandrou *et al.*, Phys. Rev. D **98** (2018) no.5, 054518 doi:10.1103/PhysRevD.98.054518 [arXiv:1807.00495 [hep-lat]].

[4] S. Aoki *et al.*, Eur. Phys. J. C **77** (2017) no.2, 112 doi:10.1140/epjc/s10052-016-4509-7 [arXiv:1607.00299 [hep-lat]].

[5] R. Frezzotti and G.C. Rossi, JHEP **0408** (2004) 007 [hep-lat/0306014].

[6] R. Frezzotti, G. Martinelli, M. Papinutto and G.C. Rossi, JHEP **0604** (2006) 038 [hep-lat/0503034].

[7] R. Frezzotti *et al.* [Alpha Collaboration], JHEP **0108** (2001) 058 [hep-lat/0101001].

[8] M. Garofalo [ETMC Collaboration], "Quark masses and decay constants in $N_f = 2 + 1 + 1$ isoQCD with Wilson clover twisted mass fermions," contribution to the Lattice '19 Conference, see https://indico.cern.ch/event/764552/contributions/3428253/attachments/1863199/3062827/Lattice2019_Garofalo.pdf

[9] C. McNeile and C. Michael [UKQCD Collaboration], Phys. Rev. D **73** (2006) 074506 [hep-lat/0603007].

[10] N. Carrasco *et al.* [ETM Coll.], Nucl. Phys. B **887** (2014) 19 [arXiv:1403.4504 [hep-lat]].

[11] J. Hardy and I. S. Towner, PoS CKM **2016** (2016) 028. doi:10.22323/1.291.0028

[12] A. Bazavov *et al.* [MILC Collaboration], Phys. Rev. D **93** (2016) no.9, 094510 doi:10.1103/PhysRevD.93.094510 [arXiv:1503.02769 [hep-lat]].

[13] S. Aoki *et al.* [Flavour Lattice Averaging Group], arXiv:1902.08191 [hep-lat].

[14] R. Baron *et al.* [ETM Collaboration], PoS LATTICE **2010** (2010) 123 doi:10.22323/1.105.0123 [arXiv:1101.0518 [hep-lat]].

Note on a SU(3) ChPT analysis of f_π, f_K and f_K/f_π using $N_f = 2+1+1$ Wilson Clover twisted-mass fermions

by Silvano

June 28, 2019

1 Partially quenched SU(3) ChPT

In this note we consider the decay constant of a pseudoscalar (PS) meson, composed by two valence quarks with masses m_1 and m_2, calculated adopting the ETMC ensembles with $N_f = 2+1+1$ Wilson Clover twisted-mass fermions, which include the physical pion point. We will denote by $m_\ell = m_u = m_d$ the sea light-quark mass (isoQCD) and by $m_s(m_c)$ the strange(charm) one.

Within partially quenched SU(3) Chiral Perturbation Theory (SU(3) ChPT) the PS decay constant $f_{m_\ell m_s}(m_1, m_2)$ is given at next-to-leading-order (NLO) by (see Eq. (30) of Ref. [1])

$$\begin{aligned} f_{m_\ell m_s}(m_1,m_2) &= f_0\Big\{1 + (4\pi)^2\left[8L_4^r(4\pi f_0)(2\xi_\ell+\xi_s) + 4L_5^r(4\pi f_0)(\xi_1+\xi_2)\right] \\ &+ \chi_{\xi_\ell\xi_s}(\xi_1,\xi_2)\Big\} \end{aligned} \tag{1}$$

where $\chi_{\xi_\ell\xi_s}(\xi_1,\xi_2)$ represents the contribution of the chiral logs

$$\begin{aligned} \chi_{\xi_\ell\xi_s}(\xi_1,\xi_2) &= \frac{1}{3}\left[\overline{A}(\xi_1)R_1^\eta + \overline{A}(\xi_2)R_2^\eta\right] - \frac{1}{6}\left[\overline{A}(\xi_1)R_1^c + \overline{A}(\xi_2)R_2^c\right] \\ &- \frac{1}{6}\overline{A}(\xi_\eta)R_\eta^v + \overline{A}\left(\frac{\xi_\ell+\xi_1}{2}\right) + \overline{A}\left(\frac{\xi_\ell+\xi_2}{2}\right) \\ &+ \frac{1}{2}\overline{A}\left(\frac{\xi_s+\xi_1}{2}\right) + \frac{1}{2}\overline{A}\left(\frac{\xi_s+\xi_2}{2}\right) \\ &- \frac{1}{6}\frac{d\overline{A}(\xi_1)}{d\xi_1}R_1^d - \frac{1}{6}\frac{d\overline{A}(\xi_2)}{d\xi_2}R_2^d \end{aligned} \tag{2}$$

and

$$\xi_\ell \equiv \frac{2B_0}{(4\pi f_0)^2} m_\ell \ , \tag{3}$$

$$\xi_s \equiv \frac{2B_0}{(4\pi f_0)^2} m_s \ , \tag{4}$$

$$\xi_{1(2)} \equiv \frac{2B_0}{(4\pi f_0)^2} m_{1(2)} \ , \tag{5}$$

$$\xi_\eta \equiv \frac{\xi_\ell + 2\xi_s}{3} \ , \tag{6}$$

$$\overline{A}(\xi) \equiv -\xi \, \log(\xi) \ , \tag{7}$$

$$R^\eta_{1(2)} \equiv \frac{(\xi_{1(2)} - \xi_\ell)(\xi_{1(2)} - \xi_s)}{(\xi_{1(2)} - \xi_{2(1)})(\xi_{1(2)} - \xi_\eta)} \ , \tag{8}$$

$$R^c_{1(2)} \equiv \frac{2\xi_{1(2)} - \xi_\ell - \xi_s}{\xi_{1(2)} - \xi_\eta} - \frac{(\xi_{1(2)} - \xi_\ell)(\xi_{1(2)} - \xi_s)}{(\xi_{1(2)} - \xi_\eta)^2} \ , \tag{9}$$

$$R^v_\eta \equiv \frac{(\xi_\eta - \xi_\ell)(\xi_\eta - \xi_s)}{(\xi_1 - \xi_\eta)^2 (\xi_2 - \xi_\eta)^2} (\xi_1 - \xi_2)^2 \ , \tag{10}$$

$$R^d_{1(2)} \equiv \frac{(\xi_{1(2)} - \xi_\ell)(\xi_{1(2)} - \xi_s)}{\xi_{1(2)} - \xi_\eta} \ . \tag{11}$$

In the above equations B_0 and f_0 are the SU(3) ChPT low-energy constants (LECs) at LO, while the NLO LECs L^r_4 and L^r_5 are evaluated at a ChPT renormalization scale μ equal to $\mu = 4\pi f_0$. The change of the LECs with respect to a variation of the scale μ is governed by the corresponding anomalous dimensions. Using the ρ-meson mass M_ρ as the standard reference value, one has

$$L^r_4(M_\rho) = L^r_4(4\pi f_0) + \frac{1}{4(4\pi)^2} \log\left(\frac{4\pi f_0}{M_\rho}\right) \ , \tag{12}$$

$$L^r_5(M_\rho) = L^r_5(4\pi f_0) + \frac{3}{8(4\pi)^2} \log\left(\frac{4\pi f_0}{M_\rho}\right) \ . \tag{13}$$

For a pion-like PS meson (i.e. $m_1 = m_2 = m$) one gets

$$\begin{aligned} f_{m_\ell m_s}(m,m) &= f_0 \Big\{ 1 + (4\pi)^2 \left[8L^r_4(4\pi f_0)(2\xi_\ell + \xi_s) + 8L^r_5(4\pi f_0)\xi \right] \\ &+ 2\overline{A}\left(\frac{\xi_\ell + \xi}{2}\right) + \overline{A}\left(\frac{\xi_s + \xi}{2}\right) \Big\} \ , \end{aligned} \tag{14}$$

where $\xi \equiv 2B_0 m/(4\pi f_0)^2$. Eq. (14) is obtained taking into account that

$$\overline{A}(\xi_1)R_1^\eta + \overline{A}(\xi_2)R_2^\eta = \overline{A}(\xi_2)R_2^c + \frac{d\overline{A}(\xi_2)}{d\xi_2}R_2^d + \mathcal{O}(\xi_1 - \xi_2) \ . \tag{15}$$

In the unitary case, i.e. $m_1 = m_s$ and $m_2 = m_\ell$, Eqs. (1) and (14) reduce to the celebrated Gasser&Leutwyler formulae, namely

$$\begin{aligned} f_\pi &= f_0\Big\{1 + (4\pi)^2\left[8L_4^r(4\pi f_0)(2\xi_K + \xi_\pi) + 8L_5^r(4\pi f_0)\xi_\pi\right] \\ &+ 2\overline{A}(\xi_\pi) + \overline{A}(\xi_K)\Big\} \ , \end{aligned} \tag{16}$$

$$\begin{aligned} f_K &= f_0\Big\{1 + (4\pi)^2\left[8L_4^r(4\pi f_0)(2\xi_K + \xi_\pi) + 8L_5^r(4\pi f_0)\xi_K\right] \\ &+ \frac{3}{4}\left[\overline{A}(\xi_\pi) + 2\overline{A}(\xi_K) + \overline{A}(\xi_\eta)\right]\Big\} \ , \end{aligned} \tag{17}$$

where the LO products B_0 times the quark masses have been replaced everywhere with the appropriate meson masses

$$\xi_\ell = \frac{2B_0 m_\ell}{(4\pi f_0)^2} \to \frac{M_\pi^2}{(4\pi f_0)^2} \equiv \xi_\pi \ , \tag{18}$$

$$\frac{\xi_\ell + \xi_s}{2} = \frac{B_0(m_\ell + m_s)}{(4\pi f_0)^2} \to \frac{M_K^2}{(4\pi f_0)^2} \equiv \xi_K \ , \tag{19}$$

$$\frac{\xi_\ell + 2\xi_s}{3} \equiv \frac{2B_0(m_\ell + 2m_s)}{3(4\pi f_0)^2} \to \frac{4M_K^2 - M_\pi^2}{3(4\pi f_0)^2} = \frac{M_\eta^2}{(4\pi f_0)^2} \equiv \xi_\eta \ . \tag{20}$$

2 Finite volume effects within SU(3) ChPT

The structure of finite volume effects (FVEs) can be studied using ChPT. At NLO FVEs come entirely from the discretized sum over periodic momenta of the loop contributions.

Let's start by considering the unitary case given in the infinite volume limit, $L \to \infty$, by Eqs. (16-17). At finite volume one has

$$\begin{aligned} f_\pi(L) &= f_0\Big\{1 + (4\pi)^2\left[8L_4^r(4\pi f_0)(2\xi_K + \xi_\pi) + 8L_5^r(4\pi f_0)\xi_\pi\right] \\ &+ 2\overline{A}(\xi_\pi) + \overline{A}(\xi_K) + \Delta_{FVE}^\pi(L)\Big\} \ , \end{aligned} \tag{21}$$

$$\begin{aligned} f_K(L) &= f_0\Big\{1 + (4\pi)^2\left[8L_4^r(4\pi f_0)(2\xi_K + \xi_\pi) + 8L_5^r(4\pi f_0)\xi_K\right] \\ &+ \frac{3}{4}\left[\overline{A}(\xi_\pi) + 2\overline{A}(\xi_K) + \overline{A}(\xi_\eta)\right] + \Delta_{FVE}^K(L)\Big\} \ . \end{aligned} \tag{22}$$

The correction terms $\Delta_{FVE}^{K(\pi)}$ can be obtained from the chiral logs via the following replacement (see Appendix C of Ref. [2])

$$\overline{A}(\xi) \to -\frac{\xi}{2}\ \widetilde{g}_1(\lambda)\ , \tag{23}$$

where $\lambda \equiv ML = \sqrt{\xi}\ 4\pi f_0 L$ and

$$\widetilde{g}_1(\lambda) = 4\sum_{n=1}^{\infty} \frac{m(n)}{\sqrt{n}\lambda} K_1\left(\sqrt{n}\lambda\right) \tag{24}$$

with K_1 being a Bessel function of the second kind and $m(n)$ the multiplicities of a three-dimensional vector $\vec{n}$ having integer norm n (i.e. $m(n) = \{6, 12, 8, 6, ...\}$). At sufficiently large values of λ the Bessel function can be replaced by its asymptotic expansion, which leads to

$$\widetilde{g}_1(\lambda) \simeq 4\sqrt{\frac{\pi}{2}} \sum_{n=1}^{\infty} \frac{m(n)}{(\sqrt{n}\lambda)^{3/2}} e^{-\sqrt{n}\lambda}\ . \tag{25}$$

Thus, one has

$$\Delta_{FVE}^{\pi}(L) \ = \ -\xi_\pi \widetilde{g}_1(\lambda_\pi) - \frac{1}{2}\xi_K \widetilde{g}_1(\lambda_K)\ , \tag{26}$$

$$\Delta_{FVE}^{K}(L) \ = \ -\frac{3}{8}\left[\xi_\pi \widetilde{g}_1(\lambda_\pi) + 2\xi_K \widetilde{g}_1(\lambda_K) + \xi_\eta \widetilde{g}_1(\lambda_\eta)\right]\ , \tag{27}$$

where the quantities $\xi_{\pi,K,\eta}$ are defined in Eqs. (18-20).

In the limit $m_s >> m_\ell$ (i.e. $\lambda_K(\lambda_\eta) >> \lambda_\pi$) one has

$$\Delta_{FVE}^{\pi}(L) \ \simeq \ -\xi_\pi \widetilde{g}_1(\lambda_\pi)\ , \tag{28}$$

$$\Delta_{FVE}^{K}(L) \ \simeq \ -\frac{3}{8}\xi_\pi \widetilde{g}_1(\lambda_\pi)\ , \tag{29}$$

which coincide with the SU(2) formulae of Ref. [2] at NLO (i.e. without Luschër resummation).

Thus, in the case of partially quenched SU(3) ChPT one gets at finite volume

$$\begin{aligned} f_{m_\ell m_s}(m_1, m_2; L) \ &= \ f_0\Big\{1 + (4\pi)^2\left[8L_4^r(4\pi f_0)(2\xi_\ell + \xi_s) + 4L_5^r(4\pi f_0)(\xi_1 + \xi_2)\right] \\ &+ \ \chi_{\xi_\ell\xi_s}(\xi_1, \xi_2) + \Delta_{FVE}(L)\Big\}\ , \end{aligned} \tag{30}$$

where $\Delta_{FVE}(L)$ can be obtained from Eq. (2) using the replacement (23) and

$$\frac{d\overline{A}(\xi)}{d\xi} \to -\frac{1}{2}\widetilde{g}_1(\lambda) - \frac{\lambda}{4}\frac{d\widetilde{g}_1(\lambda)}{d\lambda} \tag{31}$$

with

$$\frac{d\widetilde{g}_1(\lambda)}{d\lambda} \simeq -4\sqrt{\frac{\pi}{2}} \sum_{n=1}^{\infty} \frac{m(n)}{(\sqrt{n}\lambda)^{3/2}} \sqrt{n}\left(1 + \frac{3}{2\sqrt{n}\lambda}\right) e^{-\sqrt{n}\lambda}\ . \tag{32}$$

3 ETMC ensembles

Some simulation details of the ETMC ensembles considered in this note are collected in Table 1. As described in Ref. [3], the twisted-mass fermion formulation was employed including a Clover term, which helps in reducing cutoff and isospin breaking effects. The Wilson mass of the two degenerate light-quarks is chosen in order to guarantee automatic $\mathcal{O}(a)$-improvement, while the twisted masses of the heavier strange and charm quarks are tuned to their physical values.

ensemble	β	V/a^4	w_0/a	$a\mu_\ell$	$a\mu_{1(2)}$	M_π (MeV)	M_K (MeV)	L (fm)	$M_\pi L$
cA40.24	1.726	$24^3 \times 48$	1.8347(52)	0.00400	$\{a\mu_\ell, 0.0176,$	306(14)	542(16)	2.24	3.47
cA53.24		$24^3 \times 48$		0.00530	$0.0220, 0.0264\}$	351(14)	556(18)	2.24	3.99
cA30.32		$32^3 \times 64$		0.00300		267(11)	532(19)	2.99	4.04
cA12.48		$48^3 \times 96$		0.00120		170(6)	510(13)	4.48	3.85
cB25.48	1.778	$48^3 \times 96$	2.1331(47)	0.00250	$\{a\mu_\ell, 0.0148,$	257(8)	518(12)	3.86	5.03
cB07.64		$64^3 \times 128$		0.00072	$0.0185, 0.0222\}$	140(3)	493(4)	5.14	3.64
cC06.80	1.836	$80^3 \times 160$	2.4988(34)	0.00060	$\{a\mu_\ell, 0.0128,$	136(5)	493(10)	5.49	3.78
					$0.0161, 0.0193\}$				

Table 1: *Summary of the simulated light-quark sea bare mass, $a\mu_\ell$, of the four values of the valence quark bare mass, $a\mu_{1(2)}$, of the π- and K-meson masses, of the lattice size L and of the product $M_\pi L$ for the various ETMC gauge ensembles used in this note. The bare masses of the strange and charm quarks in the sea are tuned to be at their physical values [3]. In the fourth column the values estimated by ETMC [4] for the gradient-flow scale in lattice units, w_0/a, are shown. The absolute scale is set adopting for the gradient flow w_0 the value $w_0 = 0.1714$ (15) fm from Ref. [5]. The values of M_π correspond to the ground-state mass of the PS meson with $a\mu_1 = a\mu_2 = a\mu_\ell$, while the values of M_K refers to the case $a\mu_2 = a\mu_\ell$ and $a\mu_1$ equal to the third value of the set shown in the sixth column.*

In what follows the prescription which defines our isoQCD (in the light and strange sectors) is based on the following three inputs

$$M_\pi^{isoQCD} = 134.8\ (3)\ \text{MeV}\ , \tag{33}$$

$$M_K^{isoQCD} = 494.2\ (3)\ \text{MeV}\ , \tag{34}$$

$$w_0 = 0.1714\ (5)\ \text{fm}\ , \tag{35}$$

where the first two are the physical values of M_π and M_K in isoQCD recommended by FLAG-3 [6], while the third one is the gradient-flow value obtained at $N_f = 2+$

$1+1$ in Ref. [5][1]. Note that for the ensembles cB07.64 and cC06.80, corresponding respectively to a lattice spacing equal to $a \simeq 0.080$ and $a \simeq 0.069$ fm, the pion and kaon masses are simulated very close to the FLAG-3 values (33-34).

For each ensemble we compute the 2-point PS-PS correlator given by

$$C(t) = \frac{1}{L^3} \sum_{x,z} \langle 0 |\, P_5(x) P_5^\dagger(z)\, |0\rangle\, \delta_{t,(t_x - t_z)} \ , \tag{36}$$

where $P_5(x) = \overline{q}_2(x)\gamma_5 q_1(x)$ is a local interpolating PS field. The Wilson parameters of the two valence quarks q_1 and q_2 are always chosen to have opposite values. In this way the squared PS meson mass differs from its continuum counterpart only by terms of $\mathcal{O}(a^2\mu)$ [7, 8].

At large time distances one has

$$C(t) \xrightarrow[t \gg a,\ (T-t) \gg a]{} \frac{\mathcal{Z}_{PS}}{2M_{PS}} \left[e^{-M_{PS} t} + e^{-M_{PS}(T-t)} \right] \ , \tag{37}$$

so that the meson mass M_{PS} and the matrix element $\mathcal{Z}_{PS} = |\langle PS | \overline{q}_2 \gamma_5 q_1 | 0 \rangle|^2$ can be extracted from the exponential fit given in the r.h.s. of Eq. (37). The time intervals $[t_{min}, t_{max}]$ adopted for the fit (37) of the PS-PS correlation functions are collected in Table 2.

ensemble	β	V/a^4	$[t_{\rm min}/a,\ t_{\rm max}/a]$ $m_{1(2)} = m_\ell$	$[t_{\rm min}/a,\ t_{\rm max}/a]$ $m_{1,2} > m_\ell$
cA40.24	1.726	$24^3 \times 48$	[13, 22]	[16, 22]
cA53.24		$24^3 \times 48$	[13, 22]	[16, 22]
cA30.32		$32^3 \times 64$	[13, 28]	[16, 28]
cA12.48		$48^3 \times 96$	[13, 40]	[16, 40]
cB25.48	1.778	$48^3 \times 96$	[14, 40]	[18, 40]
cB07.64		$64^3 \times 128$	[14, 56]	[18, 56]
cC06.80	1.836	$80^3 \times 160$	[15, 70]	[20, 70]

Table 2: *The time intervals $[t_{min}, t_{max}]$ adopted for the fit (37) of the PS-PS correlation functions.*

For maximally twisted fermions the value of $\mathcal{Z}_{PS}$ determines the PS decay constant $f_{m_\ell m_s}(m_1, m_2)$ without the need of the knowledge of any renormalization

[1] In Ref. [5] the value of w_0 is obtained using the decay constant of a pion-like meson made of two mass-degenerate valence quarks with mass $m_\ell = 0.4 m_s$.

constant [9, 7], namely

$$af_{m_\ell m_s}(m_1, m_2) = a(\mu_1 + \mu_2)\frac{\sqrt{a^4 \mathcal{Z}_{PS}}}{aM_{PS}\,\sinh(aM_{PS})} \ . \tag{38}$$

In the case of the ensemble cA211.12.48 a correction due to a deviation from maximal twist should be applied. We use the following approximate formula

$$f_{m_\ell m_s}(m_1, m_2)|_{corrected} = f_{m_\ell m_s}(m_1, m_2) \cdot K_f \tag{39}$$

with

$$K_f \simeq \sqrt{\frac{2\kappa_1\kappa_2}{\kappa_1 + \kappa_2}} \ , \tag{40}$$

where

$$\kappa_i \equiv \sqrt{1 + (Z_A\ \mu_{PCAC}/\mu_i)^2} \ , \tag{41}$$

μ_{PCAC} is the bare PCAC mass, Z_A is the renormalization constant of the axial current and μ_i is the bare twisted mass of the valence quarks. In the pion case, where $\kappa_1 = \kappa_2 = \kappa_\ell$, the correction factor K_f becomes equal to κ_ℓ. When $m_1 >> m_2 = m_\ell$ Eq. (40) becomes $K_f \simeq \sqrt{2\kappa_\ell/(1+\kappa_\ell)} = 1/\cos(\theta_\ell/2)$, where $1/\cos(\theta_\ell) = \kappa_\ell$. For the squared PS mass the analogous correction is given by

$$M^2_{PS}(m_\ell, m_s; m_1, m_2)|_{corrected} = M^2_{PS}(m_\ell, m_s; m_1, m_2)/K_m \ , \tag{42}$$

where

$$K_m = \frac{\mu_1\kappa_1 + \mu_2\kappa_2}{\mu_1 + \mu_2} \ . \tag{43}$$

For the ensemble cA211.12.48 one has $Z_A \simeq 0.75$ and $\mu_{PCAC}/\mu_\ell \simeq -0.21\ (5)$ [10].

The statistical accuracy of the correlator (36) is significantly improved by using the so-called "one-end" stochastic method [11], which includes spatial stochastic sources at a single time slice chosen randomly. Statistical errors on the PS-meson mass and decay constant are evaluated using the jackknife procedure.

In Fig. 1 we show the results for the pion and kaon decays constants $f_{m_\ell m_s}(m_1, m_2)$ [see Eqs. (38-39)] corresponding to the quasi-unitary setup, namely when $m_2 = m_\ell$, while $m_1 = m_\ell$ for the pion case and $m_1 \sim m_s$ for the kaon case. The setup is unitary for the light quarks, while it is close to be unitary for the strange valence quark. Note that the errors of the data (statistical + scale setting) lie in the range $0.3 \div 0.9\%$ for the pion case and $0.2 \div 0.6\%$ for the kaon one.

4 SU(3) ChPT analysis of f_π and f_K

Let's now apply the SU(3) ChPT predictions for interpolating the quasi-unitary data to the physical pion and kaon points and to extrapolate them to the continuum and infinite volume limits.

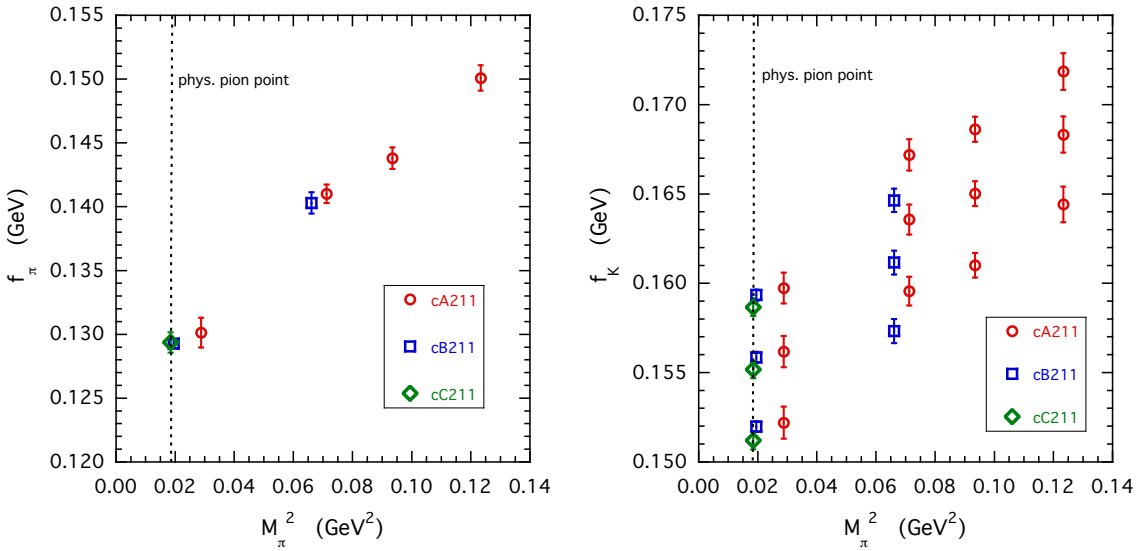

Figure 1: *Values of the decay constants* $f_{m_\ell m_s}(m_1, m_2)$ *in the quasi-unitary setup in which* $m_2 = m_\ell$*, while* $m_1 = m_\ell$ *for the pion case and* $m_1 \sim m_s$ *for the kaon case. The vertical dotted line indicates the location of the physical pion point* $(M_\pi^{phys})^2 = 0.0182$ GeV^2.

First of all we re-express the quantities ξ_ℓ, ξ_s and $\xi_{1(2)}$ (see Eqs. (3-5)) in terms of meson masses:

$$\xi_\ell = \frac{M^2_{m_\ell,m_\ell}}{(4\pi f^*)^2} = \frac{M_\pi^2}{(4\pi f^*)^2} \ , \tag{44}$$

$$\xi_s = \frac{2(M_K^{phys})^2 - (M_\pi^{phys})^2}{(4\pi f^*)^2} \ , \tag{45}$$

$$\xi_i = \frac{M^2_{m_i,m_i}}{(4\pi f^*)^2} \ , \qquad (\mathrm{i} = 1,\, 2) \tag{46}$$

where we are assuming the strange sea quark to be at its physical value and, therefore, ξ_s does not depend on the specific gauge ensemble. In Eqs. (44-46) we have replaced in the chiral logs the quantity f_0 with an effective parameter f^* to be determined in the fitting procedure. The motivation is that already the use of meson masses in Eqs. (44-46) introduces effects at higher orders in the chiral expansion. Therefore, the use of $f^* \neq f_0$ is expected to reduce further the impact of orders higher than the NLO one (as we shall see in a while).

Nevertheless, past experiences tell us that the convergence of SU(3) ChPT might be poor at NLO around the physical strange quark mass. Thus, we add to Eq. (30) terms quadratic in the quark masses (i.e., quartic in the meson masses)

as well as discretization effects, namely

$$
\begin{aligned}
f_{m_\ell m_s}(m_1,m_2) &= f_0\Big\{1+(4\pi)^2\left[8L_4^r(4\pi f^*)(2\xi_\ell+\xi_s)+4L_5^r(4\pi f^*)(\xi_1+\xi_2)\right] \\
&+ \chi_{\xi_\ell\xi_s}(\xi_1,\xi_2)+A_2^{ss}\xi_s^2+A_2^{\ell\ell}\xi_\ell^2+A_2^s\left[(\xi_1+\xi_s)^2+(\xi_2+\xi_s)^2\right] \\
&+ A_2^\ell\left[(\xi_1+\xi_\ell)^2+(\xi_2+\xi_\ell)^2\right]+A_2^-(\xi_1-\xi_2)^2+A_2^+(\xi_1+\xi_2)^2 \\
&+ \frac{a^2}{w_0^2}\left[D_s\xi_s+D_\ell\xi_\ell\right]+\Delta_{FVE}(L)\Big\}\ . \qquad (47)
\end{aligned}
$$

We start by considering the NLO fit, i.e. $A_2^i = 0$ for $i = \{ss, \ell\ell, s, \ell, -, +\}$. Surprisingly, such a fit works quite well. Moreover the FVEs are successfully taken into account using the NLO SU(3) ChPT prediction $\Delta_{FVE}(L)$, while the discretization terms can be safely put to zero (i.e. $D_s = D_\ell = 0$). The resulting $\chi^2/(\text{d.o.f.})$ is reasonable: $\chi^2/(\text{d.o.f.}) \simeq 1.3$ for 28 data points and 4 parameters. At the physical pion and kaon points in isoQCD (see Eqs. (33-35)) we get

$$
\begin{aligned}
f_\pi^{phys} &= 128.83\ (29)\ \text{MeV}\ , \qquad (48)\\
f_K^{phys} &= 155.51\ (42)\ \text{MeV}\ , \qquad (49)\\
\frac{f_K^{phys}}{f_\pi^{phys}} &= 1.2071\ (37) \qquad (50)
\end{aligned}
$$

with $f_0 = 105.0\ (1.6)$ MeV, $L_4^r(M_\rho) = 1.06\ (8)\cdot 10^{-3}$, $L_5^r(M_\rho) = 1.97\ (12)\cdot 10^{-3}$ and $f^* = 135.8\ (4.1)$ MeV. For comparison HPQCD [12] has obtained $L_4^r(M_\rho) = 0.09\ (34)\cdot 10^{-3}$ and $L_5^r(M_\rho) = 1.19\ (25)\cdot 10^{-3}$ with $N_f = 2+1+1$ dynamical quarks, while available determinations of f_0 with $N_f = 2+1$ are in the range $105 \div 120$ MeV [13].

Adding in the fitting procedure the quadratic term proportional to A_2^- the quality of the fit improves ($\chi^2/(\text{d.o.f.}) \simeq 0.8$), obtaining

$$
\begin{aligned}
f_\pi^{phys} &= 129.03\ (30)\ \text{MeV}\ , \qquad (51)\\
f_K^{phys} &= 155.55\ (39)\ \text{MeV}\ , \qquad (52)\\
\frac{f_K^{phys}}{f_\pi^{phys}} &= 1.2055\ (36) \qquad (53)
\end{aligned}
$$

with $f_0 = 111.7\ (1.8)$ MeV, $L_4^r(M_\rho) = 1.14\ (12)\cdot 10^{-3}$, $L_5^r(M_\rho) = 3.38\ (44)\cdot 10^{-3}$ and $f^* = 163.4\ (9.6)$ MeV. If we now impose the constraint $f^* = f_0$ we need to add a further quadratic term, namely the one proportional to A_2^ℓ, to keep

$\chi^2/(\text{d.o.f.}) \simeq 0.9$. In this case we get

$$f_\pi^{phys} = 128.98\ (28)\ \text{MeV}\ , \tag{54}$$

$$f_K^{phys} = 155.51\ (39)\ \text{MeV}\ , \tag{55}$$

$$\frac{f_K^{phys}}{f_\pi^{phys}} = 1.2057\ (34) \tag{56}$$

with $f_0 = 116.2\ (1.7)$ MeV, $L_4^r(M_\rho) = 0.30\ (3)\cdot 10^{-3}$, $L_5^r(M_\rho) = 0.91\ (3)\cdot 10^{-3}$ and $f^* = f_0$.

Finally, we include further data points corresponding to both m_1 and m_2 close to the physical strange quark mass (i.e. one of the three heavier masses in the set shown in the sixth column of Table 1). We obtain a total of 70 data points taking into account that $f_{m_\ell m_s}(m_1, m_2) = f_{m_\ell m_s}(m_2, m_1)$. The data added to the quasi-unitary ones correspond to large, unphysical values of both $M^2_{m_1,m_2}$ and $M^2_{m_2,m_2}$, which correspond to M_K^2 and M_π^2, respectively. Even more surprisingly than before, it is enough to add to the NLO SU(3) fit only the quadratic term proportional to A_2^- to get $\chi^2/(\text{d.o.f.}) \simeq 0.8$. No discretization terms are required. At the physical isoQCD point the results are

$$f_\pi^{phys} = 128.90\ (26)\ \text{MeV}\ , \tag{57}$$

$$f_K^{phys} = 155.45\ (41)\ \text{MeV}\ , \tag{58}$$

$$\frac{f_K^{phys}}{f_\pi^{phys}} = 1.2060\ (33) \tag{59}$$

with $f_0 = 107.2\ (1.4)$ MeV, $L_4^r(M_\rho) = 1.13\ (7)\cdot 10^{-3}$, $L_5^r(M_\rho) = 2.54\ (8)\cdot 10^{-3}$ and $f^* = 146.2\ (2.9)$ MeV.

The quality of the above fit is illustrated in Fig. 2 for the quasi-unitary data of f_π and f_K. We remind that the fitting procedure include also data at much higher values of the pion and kaon masses.

It can be seen that the SU(3) fit is able to reproduce the data except those corresponding to the ensemble cA211.12.48, which is the one affected by the maximal twist correction (40). We have therefore excluded the above data from the fitting procedure. The impact turns out to be very marginal, namely

$$f_\pi^{phys} = 128.98\ (28)\ \text{MeV}\ , \tag{60}$$

$$f_K^{phys} = 155.56\ (39)\ \text{MeV}\ , \tag{61}$$

$$\frac{f_K^{phys}}{f_\pi^{phys}} = 1.2060\ (34) \tag{62}$$

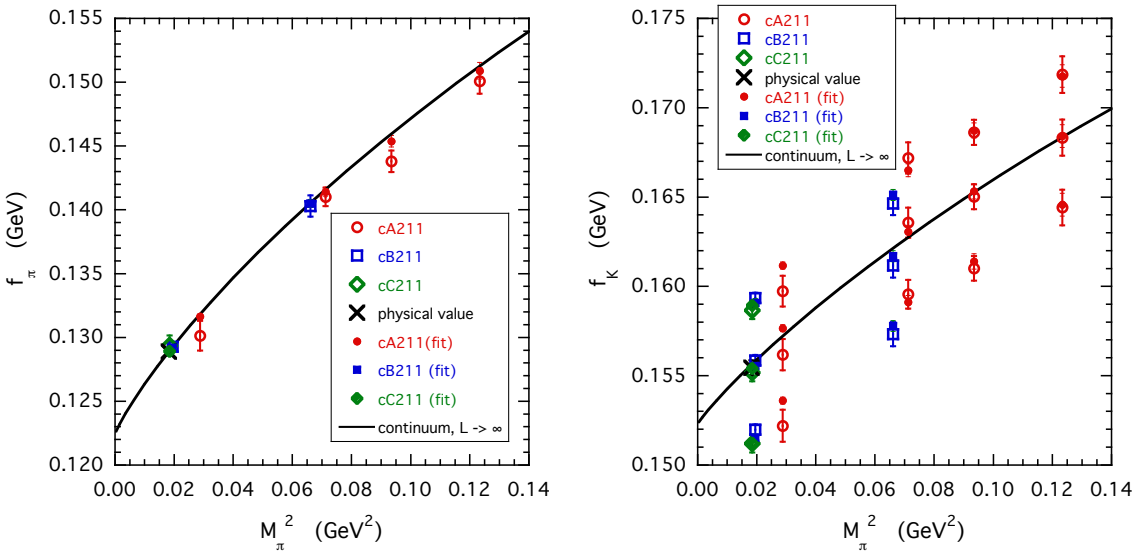

Figure 2: *The same data points as those in Fig. 1 (open markers) compared with the results of the NNLO ChPT fit (47) leading to the results (57-59) at the physical isoQCD point (full markers). The solid lines represent the continuum and infinite volume limits of Eq. (47) evaluated for f_π and f_K in the unitary case.*

with $f_0 = 107.6\ (1.4)$ MeV, $L_4^r(M_\rho) = 1.13\ (7) \cdot 10^{-3}$, $L_5^r(M_\rho) = 2.57\ (9) \cdot 10^{-3}$ and $f^* = 147.0\ (3.1)$ MeV.

In Fig. 3 all the data used for f_π (open markers) are shown together with the results of the fitting procedure (full markers). The reproduction of the data at unphysically higher values of the pion mass is very good. The differences between such data points and the solid line, representing the continuum and infinite volume limits in the unitary case, are due to the partial quenching between the heavy valence quark mass $m_1 = m_2 \simeq m_s$ and the light sea quark mass $m_\ell << m_s$. The NLO SU(3) chiral logs, given by Eq. (2), reproduce properly such differences.

We now estimate the error budget including the systematic uncertainties related to the chiral interpolation, continuum and infinite volume limits and to the errors on the scale setting. With respect to the fit leading to Eqs. (57-59) we separately consider

- the addition of the discretization terms proportional to D_s and D_ℓ;
- the addition of a factor multiplying $\Delta_{FVE}(L)$;
- the inclusion of the quadratic terms proportional to A_2^s, A_2^ℓ and A_2^+;
- the exclusion of the uncertainties of w_0/a shown in Table 1 and the error of w_0.

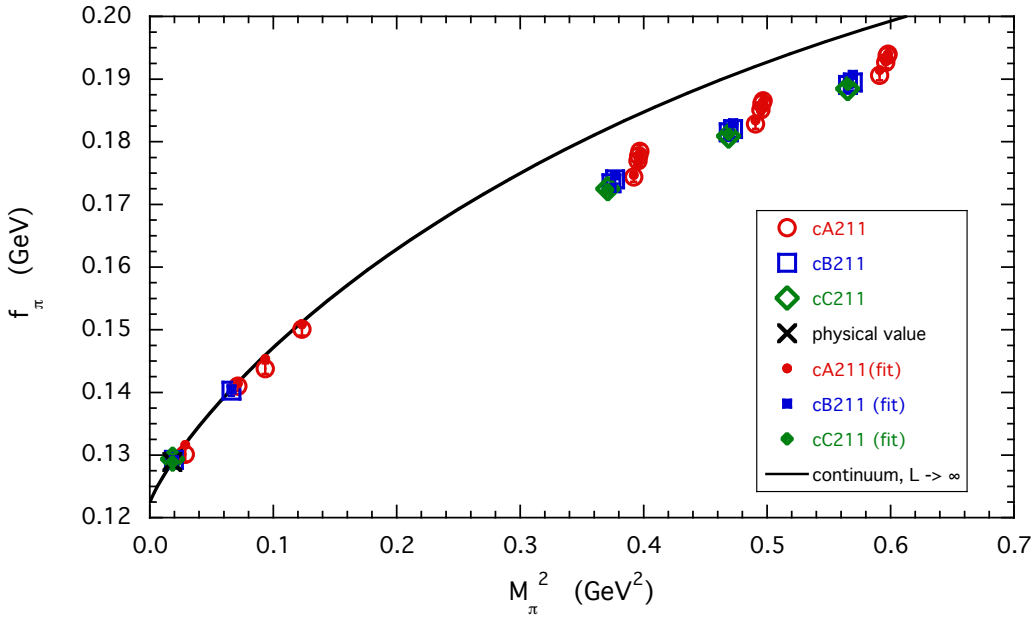

Figure 3: *The same as in the left panel of Fig. 2, but for all the data of f_π used in the fitting procedure.*

Half of the differences with respect to the results (57-59) are used as estimates of the corresponding systematic errors. We get

$$\begin{aligned} f_\pi^{phys} &= 128.90\ (10)_{\rm stat+fit}\ (24)_{\rm input}\ (5)_{\rm chir}\ (20)_{\rm disc}\ (11)_{\rm FVE}\ {\rm MeV}\ , \\ &= 128.90\ (26)_{\rm stat+fit+input}\ (23)_{\rm syst}\ {\rm MeV}\ , \\ &= 128.90\ (35)\ {\rm MeV}\ , \end{aligned} \tag{63}$$

$$\begin{aligned} f_K^{phys} &= 155.45\ (16)_{\rm stat+fit}\ (38)_{\rm input}\ (7)_{\rm chir}\ (23)_{\rm disc}\ (5)_{\rm FVE}\ {\rm MeV}\ , \\ &= 155.45\ (41)_{\rm stat+fit+input}\ (24)_{\rm syst}\ {\rm MeV}\ , \\ &= 155.45\ (48)\ {\rm MeV} \end{aligned} \tag{64}$$

and

$$\begin{aligned} \frac{f_K^{phys}}{f_\pi^{phys}} &= 1.2060\ (18)_{\rm stat+fit}\ (28)_{\rm input}\ (1)_{\rm chir}\ (1)_{\rm disc}\ (7)_{\rm FVE}\ , \\ &= 1.2060\ (33)_{\rm stat+fit+input}\ (7)_{\rm syst}\ , \\ &= 1.2060\ (34)\ . \end{aligned} \tag{65}$$

For comparison the corresponding FLAG-4 averages [13] are: $f_\pi^{phys} = 130.2\ (8)$ MeV ($N_f = 2+1$), $f_K^{phys} = 156.1\ (3)$ MeV ($N_f = 2+1+1$) and $(f_K/f_\pi)^{phys} = 1.1966\ (18)$ ($N_f = 2+1+1$), which correspond respectively to a deviation of $\simeq 1.6$, $\simeq 1.1$ and $\simeq 2.5$ standard deviations.

However, one should keep in mind that our isoQCD results are defined in the prescription given by Eqs. (33-35). The difference between our value (63) for f_π^{phys} and the corresponding FLAG-4 average seems to indicate that our and the FLAG-based schemes defining isoQCD are different beyond the current level of precision.

Before closing this Section, we perform a simple test on the prescription dependence of our results (63-65). For sake of simplicity we consider the fitting ansatz leading to Eqs. (57-59), but now we replace Eq. (35) with $w_0 = 0.1693\ (15)$ fm (which represents a $\simeq 1.2\%$ reduction). We get

$$f_\pi^{phys} = 130.36\ (26)\ \text{MeV}\ , \tag{66}$$

$$f_K^{phys} = 156.85\ (42)\ \text{MeV}\ , \tag{67}$$

$$\frac{f_K^{phys}}{f_\pi^{phys}} = 1.2031\ (33) \tag{68}$$

with $f_0 = 108.7\ (1.4)$ MeV, $L_4^r(M_\rho) = 1.15\ (7)\cdot 10^{-3}$, $L_5^r(M_\rho) = 2.57\ (8)\cdot 10^{-3}$ and $f^* = 148.2\ (2.8)$ MeV. With the modified value of w_0 the pion decay constant at the physical isoQCD point is now very close to the (pseudo-)experimental value $f_\pi = 130.4\ (2)$ MeV, which, together with the pion and kaon masses given by Eqs. (33-34), defines the FLAG-based scheme adopted by ETMC in Ref. [14]. It can be seen that, while the values of both f_π^{phys} and f_K^{phys} change well above the uncertainties, the ratio f_K^{phys}/f_π^{phys} changes only by approximately one standard deviation.

5 Ratio of decay constants

We construct the following ratio of PS decay constants

$$R_{m_\ell m_s}(m_1, m_2) \equiv \frac{f_{m_\ell m_s}(m_1, m_2)}{f_{m_\ell m_s}(m_2, m_2)}\ . \tag{69}$$

The NLO SU(3) ChPT prediction for $R_{m_\ell m_s}(m_1, m_2)$ is given by

$$R_{m_\ell m_s}(m_1, m_2) = 1 + (4\pi)^2 4 L_5^r (4\pi f_0)(\xi_1 - \xi_2) + \overline{\chi}_{\xi_\ell \xi_s}(\xi_1, \xi_2)\ , \tag{70}$$

where only the contribution from the LEC L_5^r survives and the chiral logs are now given by

$$\overline{\chi}_{\xi_\ell \xi_s}(\xi_1, \xi_2) \equiv \chi_{\xi_\ell \xi_s}(\xi_1, \xi_2) - \chi_{\xi_\ell \xi_s}(\xi_2, \xi_2)$$

$$
\begin{aligned}
&= \frac{1}{3}\left[\overline{A}(\xi_1)R_1^\eta + \overline{A}(\xi_2)R_2^\eta\right] - \frac{1}{6}\left[\overline{A}(\xi_1)R_1^c + \overline{A}(\xi_2)R_2^c\right] \\
&- \frac{1}{6}\overline{A}(\xi_\eta)R_\eta^v + \overline{A}\left(\frac{\xi_\ell+\xi_1}{2}\right) - \overline{A}\left(\frac{\xi_\ell+\xi_2}{2}\right) \\
&+ \frac{1}{2}\overline{A}\left(\frac{\xi_s+\xi_1}{2}\right) - \frac{1}{2}\overline{A}\left(\frac{\xi_s+\xi_2}{2}\right) \\
&- \frac{1}{6}\frac{d\overline{A}(\xi_1)}{d\xi_1}R_1^d - \frac{1}{6}\frac{d\overline{A}(\xi_2)}{d\xi_2}R_2^d \ . \qquad (71)
\end{aligned}
$$

Note that thanks to Eq. (15) one has $\overline{\chi}_{\xi_\ell\xi_s}(\xi_1,\xi_2) = \mathcal{O}(\xi_1-\xi_2)$ and therefore $R_{m_\ell m_s}(m_1,m_2) = 1 + \mathcal{O}(\xi_1-\xi_2)$.

At finite volume one gets

$$
\begin{aligned}
R_{m_\ell m_s}(m_1,m_2;L) &= 1 + (4\pi)^2 4L_5^r(4\pi f_0)(\xi_1-\xi_2) + \overline{\chi}_{\xi_\ell\xi_s}(\xi_1,\xi_2) \\
&+ \overline{\Delta}_{FVE}(L) \ , \qquad (72)
\end{aligned}
$$

where $\overline{\Delta}_{FVE}(L)$ can be obtained from Eq. (71) using the replacements (23) and (31).

In the unitary case, i.e. $m_1 = m_s$ and $m_2 = m_\ell$, Eq. (72) reduces to the well-known Gasser&Leutwyler formula

$$
\begin{aligned}
\frac{f_K}{f_\pi} &= 1 + (4\pi)^2 8L_5^r(4\pi f_0)(\xi_K-\xi_\pi) - \frac{1}{4}\left[5\overline{A}(\xi_\pi) - 2\overline{A}(\xi_K) - 3\overline{A}(\xi_\eta)\right] \\
&+ \Delta_{FVE}^K(L) - \Delta_{FVE}^\pi(L) \qquad (73)
\end{aligned}
$$

with

$$
\Delta_{FVE}^K(L) - \Delta_{FVE}^\pi(L) = \frac{1}{8}\left[5\xi_\pi\widetilde{g}_1(\lambda_\pi) - 2\xi_K\widetilde{g}_1(\lambda_K) - 3\xi_\eta\widetilde{g}_1(\lambda_\eta)\right] \ , \qquad (74)
$$

In the limit $m_s >> m_\ell$ (i.e. $\lambda_K(\lambda_\eta) >> \lambda_\pi$) one has

$$
\Delta_{FVE}^K(L) - \Delta_{FVE}^\pi(L) \simeq \frac{5}{8}\xi_\pi\widetilde{g}_1(\lambda_\pi) \ , \qquad (75)
$$

which represents the SU(2) formulae of Ref. [2] at NLO (i.e. without Luschër resummation).

6 SU(3) ChPT analysis of the decay constant ratio

The results for the ratio $R_{m_\ell m_s}(m_1,m_2)$ (see Eq. (69)) corresponding to the quasi-unitary setup are shown in Fig. 4. Note that the statistical errors of the data lie in the range $0.1 \div 0.5\%$.

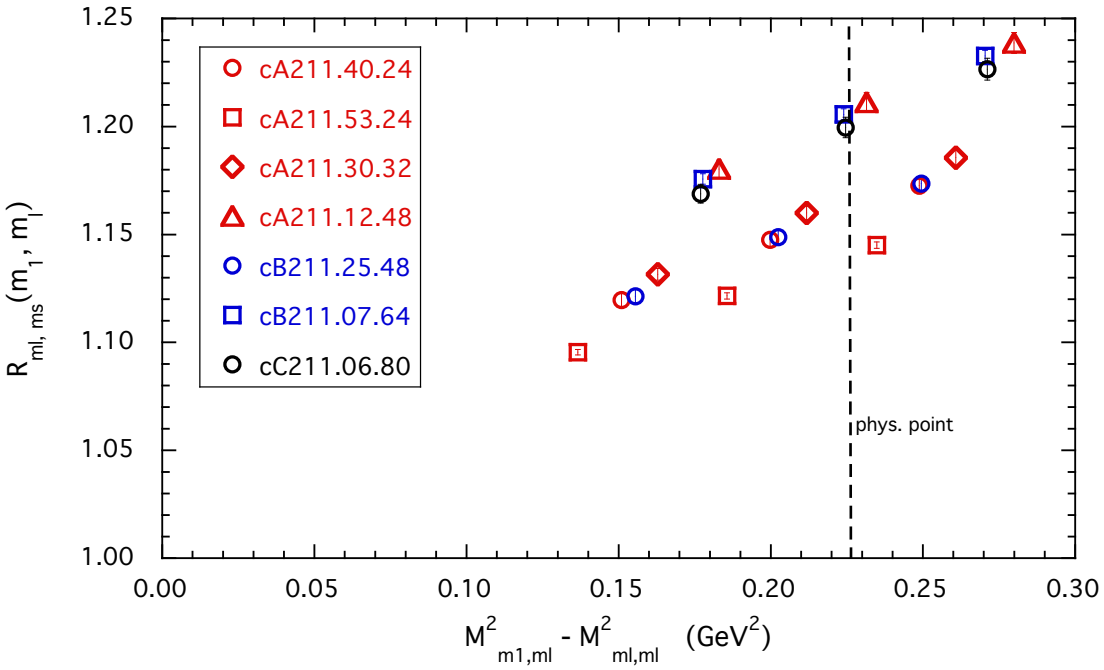

Figure 4: *Values of the decay constant ratio $R_{m_\ell m_s}(m_1, m_2)$ in the quasi-unitary setup in which $m_2 = m_\ell$ and $m_1 \sim m_s$. The vertical dashed line indicates the location of the physical isoQCD point $(M_K^{isoQCD})^2 - (M_\pi^{isoQCD})^2 \simeq 0.2261$ GeV^2.*

As in the cases of f_π and f_K, we add to the NLO SU(3) ChPT prediction (72) for the ratio $R_{m_\ell m_s}(m_1, m_\ell)$ terms quadratic in the quark masses as well as discretization effects, keeping the proportionality to $(\xi_1 - \xi_\ell)$ (since $R = 1$ when $\xi_1 = \xi_\ell$). The fitting ansatz is:

$$\begin{aligned} R_{m_\ell m_s}(m_1, m_\ell; L) &= 1 + (4\pi)^2 4L_5^r(4\pi f^*)(\xi_1 - \xi_\ell) + \overline{\chi}_{\xi_\ell\xi_s}(\xi_1, \xi_\ell) \\ &+ (\xi_1 - \xi_\ell)\left[B_2^\ell \xi_\ell + B_2^-(\xi_1 - \xi_\ell) + B_2^+(\xi_1 + \xi_\ell)\right] \\ &+ \frac{a^2}{w_0^2}(\xi_1 - \xi_\ell)\left[D_1 + D_2^\ell \xi_\ell\right] + \overline{\Delta}_{FVE}(L) \ , \end{aligned} \tag{76}$$

where $\overline{\Delta}_{FVE}(L)$ is constructed from $\overline{\chi}_{\xi_\ell\xi_s}(\xi_1, \xi_\ell)$ as explained in Section 2. In Eq. (76) there are seven free parameters, L_5^r, f^*, B_2^ℓ, B_2^-, B_2^+, D_1 and D_2^ℓ to be fitted against 21 data.

Let's start by considering the ansatz suggested by the results of the previous Section, namely let's put $D_1 = D_2^\ell = 0$ and all $B_i = 0$ except B_2^- for a total of only 3 parameters. The resulting χ^2/(d.o.f.) is acceptable, χ^2/(d.o.f.) $\simeq 1.4$, and

the result at the physical isoQCD point is

$$\left(\frac{f_K}{f_\pi}\right)^{phys} = 1.2056\ (29) \tag{77}$$

with $L_5^r(M_\rho) = 1.62\ (11) \cdot 10^{-3}$ and $f^* = 139.6\ (2.9)$ MeV. The value (77) agrees well with Eq. (65) both for the central value and for the error.

However, if the parameter D_1 is switched on, the value of $\chi^2/(\text{d.o.f.})$ decreases significantly down to $\simeq 0.69$ and the result at the physical isoQCD point becomes

$$\left(\frac{f_K}{f_\pi}\right)^{phys} = 1.1874\ (123) \tag{78}$$

with $L_5^r(M_\rho) = 1.20\ (26) \cdot 10^{-3}$ and $f^* = 133.0\ (4.6)$ MeV.

Thus, discretization effects appear to have an important impact on the continuum extrapolation of the decay constant ratio. The uncertainty of the result (78) is clearly unsatisfactory, because it is almost 3-4 times the typical statistical error of the data. A closer inspection reveals that the problem lies in the following combination of parameters, $(4\pi)^2 4L_5^r + D_1 a^2/w_0^2$, that governs the slope of the decay constant ratio in terms of the variable $(\xi_1 - \xi_\ell)$ at fixed lattice spacing. While such a combination is well determined (with an uncertainty much less than the percent), the two separate parameters L_5^r and D_1 are anticorrelated, so that their individual uncertainties are much larger. In this way, once the continuum limit is performed, the error of the decay constant ratio blows up.

In order to improve the accuracy of the determination of $(f_K/f_\pi)^{phys}$ a possible strategy is to add data in the region of small values of the variable $M^2_{m_1,m_2} - M^2_{m_2,m_2}$. This can be done by simulating values of the valence strange mass closer to the light-quark one. In absence of such data we can use the results available when both m_1 and m_2 are close to the physical value of the strange quark mass. In this way small values of the variable $M^2_{m_1,m_2} - M^2_{m_2,m_2}$ (corresponding to $M_K^2 - M_\pi^2$) can be reached at the price of dealing with data at large, unphysical values of the sum $M^2_{m_1,m_2} + M^2_{m_2,m_2}$ (corresponding to $M_K^2 + M_\pi^2$).

A total of 84 data, shown in Fig. 5, are obtained: 42 data correspond to positive values of $M^2_{m_1,m_2} - M^2_{m_2,m_2}$ and other 42 to negative values, since $R_{m_\ell m_s}(m_1, m_2) \neq R_{m_\ell m_s}(m_2, m_1)$ for $m_1 \neq m_2$. The comparison with Fig. 4 shows that 21 data are added at values of $M^2_{m_1,m_2} - M^2_{m_2,m_2}$ close to $\simeq 0.05$ and $\simeq 0.10$ GeV^2 (corresponding roughly to $m_{1(2)}/m_\ell \simeq 1.25$ and 1.5). The statistical errors of the new data are extremely small, almost an order of magnitude less than the errors of the quasi-unitary data.

In order to take into account the data at large values of $M^2_{m_1,m_2} + M^2_{m_2,m_2}$, we include in the fitting ansatz more polynomial terms (up to the cubic ones in the

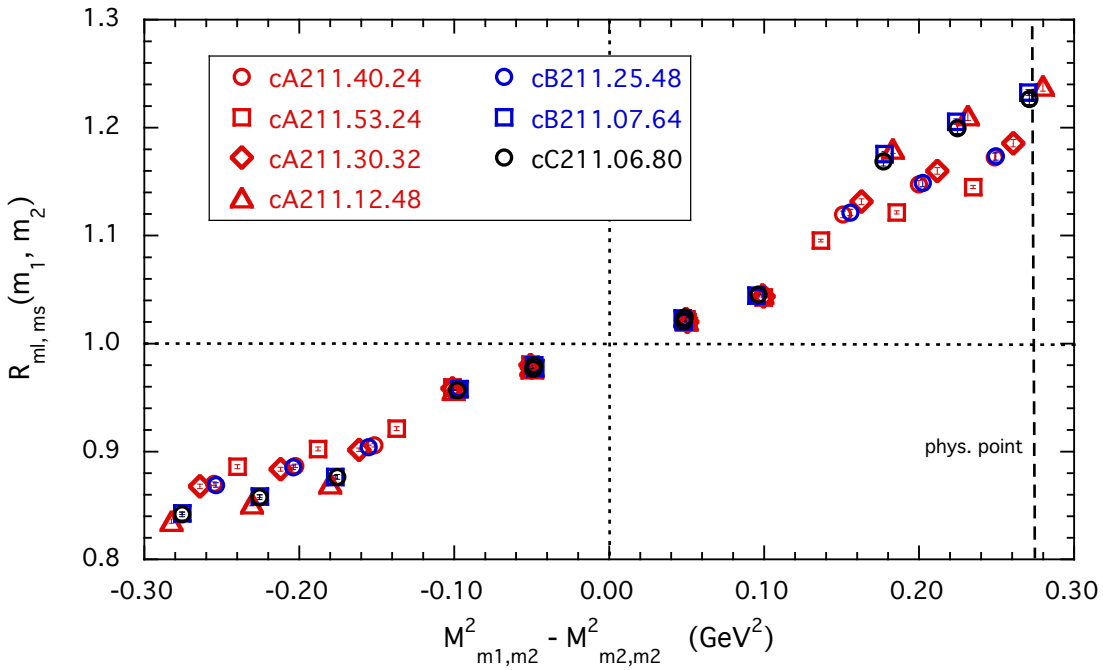

Figure 5: *Values of the decay constant ratio $R_{m_\ell m_s}(m_1, m_2)$ for all possible combinations of the valence quark masses m_1 and m_2 of Table 1.*

quark masses), namely

$$
\begin{aligned}
R_{m_\ell m_s}(m_1, m_2; L) &= 1 + (4\pi)^2 4L_5^r(4\pi f^*)(\xi_1 - \xi_2) + \overline{\chi}_{\xi_\ell \xi_s}(\xi_1, \xi_2) \\
&+ (\xi_1 - \xi_2)\left[B_2^\ell \xi_\ell + B_2^-(\xi_1 - \xi_2) + B_2^+(\xi_1 + \xi_2)\right] \\
&+ (\xi_1 - \xi_2)\left[B_3^{\ell\ell}\xi_\ell^2 + B_3^2(\xi_1 + \xi_2)^2\right] \\
&+ (\xi_1 - \xi_2)^2\left[B_3^\ell \xi_\ell + B_3^-(\xi_1 - \xi_2) + B_3^+(\xi_1 + \xi_2)\right] \\
&+ \frac{a^2}{w_0^2}(\xi_1 - \xi_2)\left[D_1 + D_2^\ell \xi_\ell + D_2^-(\xi_1 - \xi_2) + D_2^+(\xi_1 + \xi_2)\right] \\
&+ \kappa_{FVE}\overline{\Delta}_{FVE}(L)\ , \qquad (79)
\end{aligned}
$$

where also a multiplicative factor κ_{FVE} has been introduced for tuning better the FVE correction. The total number of free parameters is 15, but in practice five parameters B_3^+, B_3^2, $B_3^{\ell\ell}$, D_2^- and D_2^+ can be safely put to zero, leading to a total of 10 free parameters. The quality of the fit is good, χ^2/d.o.f. $\simeq 0.95$, and for

$(f_K/f_\pi)^{phys}$ we get

$$\left(\frac{f_K}{f_\pi}\right)^{phys} = 1.1976\ (36)\ , \tag{80}$$

which agrees well with the $N_f = 2+1+1$ average $(f_K/f_\pi)^{phys} = 1.1966\ (18)$ [13], but it deviates from the result (65) of Section 4. For f^* and $L_5^r(M_\rho)$ we obtain $f^* = 119.8\ (1.5)$ MeV and $L_5^r(M_\rho) = 0.72\ (4) \cdot 10^{-3}$, respectively.

The addition of more data at low values of $M^2_{m_1,m_2} - M^2_{m_2,m_2}$ improves the uncertainty at the physical isoQCD point, which is now at the level of the one obtained in Section 4.

We stress however that the crucial parameter in the above fit is the multiplicative FVE parameter κ_{FVE}, which reaches a quite large value, namely $\kappa_{FVE} = 3.6\ (5)$. Such a value is unnatural taking into account the findings of the analyses of f_π and f_K done in Section 4. Moreover, at variance with those analyses also discretization effects are now at work in the fitting procedure. An anomalous correlation between FVEs and discretization effects seems to take place for the decay constant ratio.

If we constrain κ_{FVE} to be equal to 1, the quality of the fit deteriorates (χ^2/d.o.f. $\simeq 2.0$), but the change in $(f_K/f_\pi)^{phys}$ is within the uncertainties, namely $(f_K/f_\pi)^{phys} = 1.2008\ (37)$. However, the latter value is consistent with the result (65) of Section 4.

7 Implications for V_{us} and the first-row CKM unitarity

In Refs. [15, 16] the leading electromagnetic and strong isospin-breaking corrections to the pion and kaon leptonic decay rates have been evaluated on the lattice. There the calculations have been carried out in the GRS scheme [17] and it has been shown that to the current level of precision the GRS scheme can be considered equivalent to the FLAG-based scheme, where the pion and kaon masses are given by Eqs. (33-34), but the lattice scale is set by the (pseudo-)experimental value of $f_\pi = 130.4(2)$ MeV. As is known, the latter one is obtained assuming for the CKM matrix element V_{ud} the value coming from the analysis of super-allowed nuclear beta decays made in Ref. [18]

As already pointed out in Section 4, the FLAG-based scheme appears to be different from the scheme adopted in this note for defining isoQCD. Therefore, we do not make use of the results of Refs. [15, 16] corresponding to the separate pion and kaon leptonic decays, but we will limit ourselves to the case of their ratio, which involves the decay constant ratio f_K/f_π, which is much less sensitive to the value chosen for w_0 (see the discussion at the end of Section 4).

The ratio of kaon to pion decay rates is given by

$$\frac{\Gamma(K^\pm \to \ell^\pm \bar{\nu}_\ell[\gamma])}{\Gamma(\pi^\pm \to \ell^\pm \bar{\nu}_\ell[\gamma])} = \left(\frac{1-r_K}{1-r_\pi}\right)^2 \frac{M_{K^\pm}}{M_{\pi^\pm}} \left|\frac{V_{us}}{V_{ud}}\right|^2 \left(\frac{f_K}{f_\pi}\right)^2 \cdot (1+\delta R_{K\pi}) \ , \tag{81}$$

where $\delta R_{K\pi}$ encodes the isospin-breaking corrections, $r_{K(\pi)} = 1 - m^2_{lepton}/M^2_{K(\pi)}$ and the f_K/f_π is the decay constant ratio evaluated in isoQCD.

Using the pion and kaon experimental masses and decay rates into muons and the updated determination $\delta R_{K\pi} = -0.0126\ (14)$ one has [16]

$$\frac{|V_{us}|}{|V_{ud}|}\frac{f_K}{f_\pi} = 0.27683\ (29)_{\rm exp}\ (20)_{\rm th} = 0.27683\ (35)\ . \tag{82}$$

Using our SU(3) result (65) for f_K/f_π we find

$$\frac{|V_{us}|}{|V_{ud}|} = 0.22954\ (24)_{\rm exp}\ (67)_{\rm th} = 0.22954\ (71)\ . \tag{83}$$

Taking the updated value $|V_{ud}| = 0.97420\ (21)$ from super-allowed nuclear beta decays [18], Eq. (83) yields the following value for the CKM element $|V_{us}|$:

$$|V_{us}| = 0.22362\ (24)_{\rm exp}\ (65)_{\rm th} = 0.22362\ (69)\ , \tag{84}$$

which differs from the latest estimate $|V_{us}| = 0.2253\ (7)$ from leptonic modes, recently updated by the PDG [19], by $\simeq 1.7$ standard deviations.

Taking the values $|V_{ub}| = 0.00413(49)$ [19] and $|V_{ud}| = 0.97420(21)$ [18] our result in Eq. (84) implies that the unitarity of the first-row of the CKM matrix

$$|V_{ud}|^2 + |V_{us}|^2 + |V_{ub}|^2 = 0.99909\ (51) \tag{85}$$

holds within $\simeq 1.8$ standard deviations.

In a recent paper [20] the hadronic contribution to the electroweak radiative corrections to neutron and super-allowed nuclear β decays has been analyzed in terms of dispersion relations and neutrino scattering data. With respect to the result $V_{ud} = 0.97420\ (21)$ from Ref. [18] a significant shift in the central value and a reduction of the uncertainty have been obtained, namely $V_{ud} = 0.97370\ (14)$ [20]. The impact of the new value of V_{ud} on our determinations of V_{us} is $V_{us} = 0.22350\ (69)$, i.e. well within the uncertainties shown in Eq. (84). On the contrary, the first-row CKM unitarity (85) will be significantly modified into

$$|V_{ud}|^2 + |V_{us}|^2 + |V_{ub}|^2 = 0.99806\ (41)\ , \tag{86}$$

which would imply a $\simeq 4.7\sigma$ tension with unitarity.

Another source of information on V_{us} is represented by the semileptonic $K_{\ell 3}$ decay. In this case the relevant hadronic quantity is the vector form factor at zero momentum transfer $f_+(0)$. From the high-precision experimental data on $K_{\ell 3}$ decays one has $V_{us} f_+(0) = 0.2165\ (4)$ [21].

Using the ETMC determination $f_+(0) = 0.9709\ (46)$ from Ref. [22], one gets the interval $V_{us} = 0.2230\ (11)$, which is consistent with Eq. (84). The above interval can be combined with Eq. (83) to obtain the red ellipse in Fig. 6, which represents a 68% likelihood contour. For comparison the blue ellipse corresponds to the FLAG-4 contour at $N_f = 2 + 1 + 1$ [13], while the green ellipse correspond to the use of Eq. (68) instead of Eq. (65). The two determinations of V_{ud} obtained in Refs. [18, 20] are also shown as well as the dotted line, which represents the correlation between V_{us} and V_{ud} when the CKM matrix is unitary.

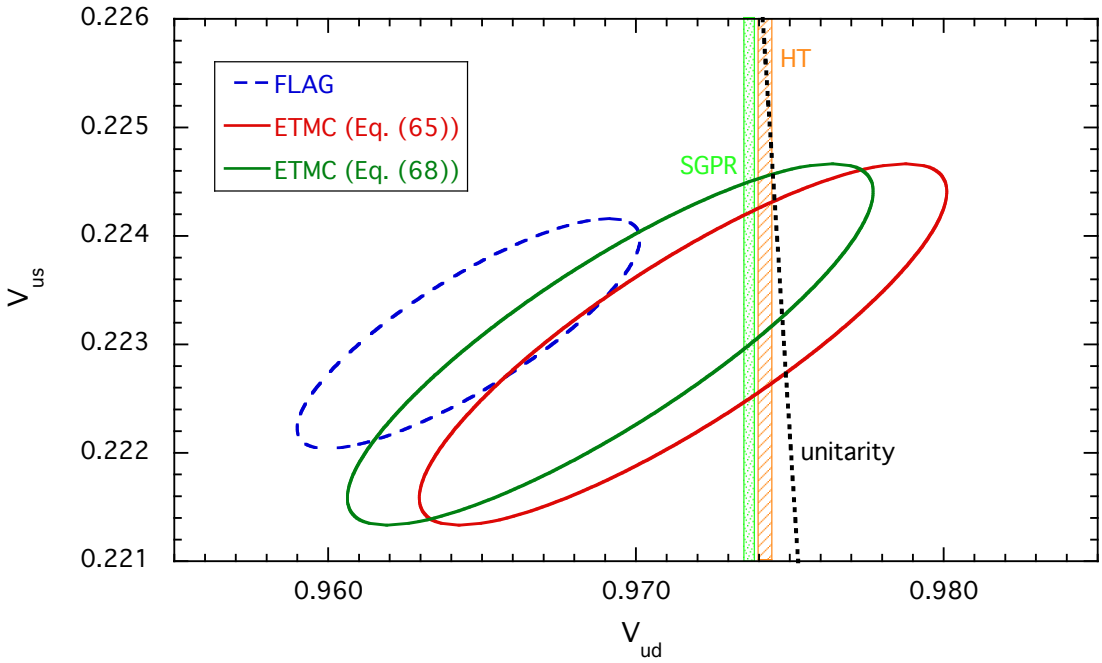

Figure 6: *The plot compares the information for V_{ud} and V_{us} obtained in the FLAG-4 review for $N_f = 2+1+1$ and in this note by ETMC using Eq. (83) and the semileptonic result of Ref. [22] or, alternatively, Eq. (68) instead of Eq. (65). The determinations of V_{ud} obtained from superallowed nuclear β transitions in Refs. [18, 20] are also shown as green and orange bands, labelled respectively HT and SGPR. The dotted line indicates the correlation between V_{ud} and V_{us} that follows if the CKM-matrix is unitary. The ellipses represent 68% likelihood contours.*

References

[1] J. Bijnens and T. A. Lahde, Phys. Rev. D **71** (2005) 094502 doi:10.1103/PhysRevD.71.094502 [hep-lat/0501014].

[2] G. Colangelo, S. Durr and C. Haefeli, Nucl. Phys. B **721** (2005) 136 doi:10.1016/j.nuclphysb.2005.05.015 [hep-lat/0503014].

[3] C. Alexandrou *et al.*, Phys. Rev. D **98** (2018) no.5, 054518 doi:10.1103/PhysRevD.98.054518 [arXiv:1807.00495 [hep-lat]].

[4] M. Garofalo et al., PRACE PLepNuGam project.

[5] A. Bazavov *et al.* [MILC Collaboration], Phys. Rev. D **93** (2016) no.9, 094510 doi:10.1103/PhysRevD.93.094510 [arXiv:1503.02769 [hep-lat]].

[6] S. Aoki *et al.*, Eur. Phys. J. C **77** (2017) no.2, 112 doi:10.1140/epjc/s10052-016-4509-7 [arXiv:1607.00299 [hep-lat]].

[7] R. Frezzotti and G.C. Rossi, JHEP **0408** (2004) 007 [hep-lat/0306014].

[8] R. Frezzotti, G. Martinelli, M. Papinutto and G.C. Rossi, JHEP **0604** (2006) 038 [hep-lat/0503034].

[9] R. Frezzotti *et al.* [Alpha Collaboration], JHEP **0108** (2001) 058 [hep-lat/0101001].

[10] M. Garofalo [ETMC Collaboration], "Quark masses and decay constants in $N_f = 2 + 1 + 1$ isoQCD with Wilson clover twisted mass fermions," contribution to the Lattice '19 Conference, see https://indico.cern.ch/event/764552/contributions/3428253/attachments/1863199/3062827/Lattice2019_Garofalo.pdf

[11] C. McNeile and C. Michael [UKQCD Collaboration], Phys. Rev. D **73** (2006) 074506 [hep-lat/0603007].

[12] R. J. Dowdall, C. T. H. Davies, G. P. Lepage and C. McNeile, Phys. Rev. D **88** (2013) 074504 doi:10.1103/PhysRevD.88.074504 [arXiv:1303.1670 [hep-lat]].

[13] S. Aoki *et al.* [Flavour Lattice Averaging Group], arXiv:1902.08191 [hep-lat].

[14] N. Carrasco *et al.* [ETM Coll.], Nucl. Phys. B **887** (2014) 19 [arXiv:1403.4504 [hep-lat]].

[15] D. Giusti, V. Lubicz, G. Martinelli, C. T. Sachrajda, F. Sanfilippo, S. Simula, N. Tantalo and C. Tarantino, Phys. Rev. Lett. **120** (2018) no.7, 072001 doi:10.1103/PhysRevLett.120.072001 [arXiv:1711.06537 [hep-lat]].

[16] M. Di Carlo, D. Giusti, V. Lubicz, G. Martinelli, C. T. Sachrajda, F. Sanfilippo, S. Simula and N. Tantalo, arXiv:1904.08731 [hep-lat].

[17] J. Gasser, A. Rusetsky, I. Scimemi, Eur. Phys. J. **C32** (2003) 97-114. [hep-ph/0305260].

[18] J. Hardy and I. S. Towner, PoS CKM **2016** (2016) 028. doi:10.22323/1.291.0028

[19] M. Tanabashi *et al.* [Particle Data Group], Phys. Rev. D **98** (2018) no.3, 030001. doi:10.1103/PhysRevD.98.030001

[20] C. Y. Seng, M. Gorchtein, H. H. Patel and M. J. Ramsey-Musolf, Phys. Rev. Lett. **121** (2018) no.24, 241804 doi:10.1103/PhysRevLett.121.241804 [arXiv:1807.10197 [hep-ph]].

[21] M. Moulson, PoS CKM **2016** (2017) 033 doi:10.22323/1.291.0033 [arXiv:1704.04104 [hep-ex]].

[22] N. Carrasco, P. Lami, V. Lubicz, L. Riggio, S. Simula and C. Tarantino, Phys. Rev. D **93** (2016) no.11, 114512 doi:10.1103/PhysRevD.93.114512 [arXiv:1602.04113 [hep-lat]].